



# Flight Test of Takeoff Performance Monitoring System

---

*David B. Middleton, Raghavachari Srivatsan, and Lee H. Person, Jr.*



# Flight Test of Takeoff Performance Monitoring System

---

*David B. Middleton*

*Langley Research Center • Hampton, Virginia*

*Raghavachari Srivatsan*

*ViGYAN, Inc. • Hampton, Virginia*

*Lee H. Person, Jr.*

*Langley Research Center • Hampton, Virginia*

The use of trademarks or names of manufacturers in this report is for accurate reporting and does not constitute an official endorsement, either expressed or implied, of such products or manufacturers by the National Aeronautics and Space Administration.

## Summary

The Takeoff Performance Monitoring System (TOPMS) has been developed at the Langley Research Center and flight tested on the Transport System Research Vehicle (TSRV), a highly modified Boeing 737-100 research airplane. The TOPMS is a computer software and hardware graphics system that visually displays current runway position, acceleration performance, engine status, and other situation advisory information to aid pilots in their decision to continue or to abort a takeoff. A total of 55 takeoff and 30 abort situations were investigated at five airfields. The TOPMS was tested for various nominal and off-nominal conditions, including normal takeoffs; reduced-throttle takeoffs; induced-acceleration deficiencies; simulated-engine failures; and several gross-weight, runway-geometry, runway-surface, and ambient conditions. All tests were made on dry runways.

Before brake release, the TOPMS algorithm generated pretakeoff-predicted performance using the nominal acceleration computed with data for the existing and/or expected conditions. Then the algorithm computed real-time performance based on measured acceleration during takeoff and compared this with the predicted performance. Additionally, the algorithm provided graphical GO/NO-GO advice (conveyed by situation advisory flags—SAF's) and continually updated the predicted position of where the airplane could be braked to a stop. Full-time symbology depicted the airplane progress and performance; advisory and predicted stop point information appeared only when dictated by the situation.

The TOPMS algorithm was programmed on the TSRV existing flight displays computer. The airplane high-speed digital autonomous terminal access communication (DATAC) system supplied the algorithm with measured data from the airplane sensors and delivered computed data to drive symbology on the airplane electronic display screens. Three sources of acceleration signals were used during the test series. The airplane body-mounted accelerometers and a gimballed inertial measuring unit (IMU) generated satisfactory TOPMS input signals. Partway through the TOPMS test series, a strap-down air data and inertial reference system (ADIRS) package replaced the IMU on the TSRV. However, the ADIRS along-track acceleration signal was so noisy that its use was discontinued after six test runs. (In postflight analysis, this signal was found to be inadequately filtered for use in the runway research operations conducted in this study.)

The flight tests demonstrated that TOPMS technology developed on the TSRV B-737 simulator had been successfully transferred to the TSRV. The TOPMS algorithm predicted runway distances with reasonable accuracy and the displays depicted the various test conditions and GO/NO-GO advisories correctly. For example, in six normal takeoff runs, most of the pretakeoff-predicted and real-time-computed distances to accelerate the airplane to takeoff speed agreed to within approximately two airplane (TSRV) lengths. A ground-based laser radar tracker at the Wallops Flight Facility continually measured the TSRV range during two of these runs and showed that the airplane position when it reached rotation speed  $V_R$  was approximately one-half of an airplane length farther down the runway than was predicted during pretakeoff computations and approximately two lengths farther than the distance computed in real time by the algorithm. Similar agreement was obtained for two runs that were aborted at approximately 80 and 100 knots on dry pavement. Postflight analysis showed that had the airplane independently measured ground speed been the basis of the computed runway distance in the two executed and two aborted takeoffs, the computed and measured distances would have been in much closer agreement.

## Introduction

In recent years, airplane safety has shown improvement in all segments of flight except during takeoff or abort situations. According to the National Transportation Safety Board (NTSB) records, more than 4000 takeoff-related accidents occurred between 1983 and 1990 that resulted in 1378 fatalities. Among large airliners, 8.7 percent of all accidents occurred during takeoff or abort situations; for regional airliners, 12.5 percent occurred during this critical phase. (See ref. 1.)

Current flight management systems do not comprehensively or effectively monitor airplane performance on the runway. In particular, they do not provide pilots with timely knowledge of their measured along-track acceleration relative to a computed nominal acceleration based on existing conditions and standard (i.e., ideal) execution of the takeoff-roll maneuver. They also do not provide explicit advisory GO/NO-GO decision aids during the takeoff roll. (See ref. 2.) Thus, many serious takeoff-related accidents might be precluded or downgraded to relatively safe, low-speed aborted takeoffs if an appropriate takeoff performance monitoring system were available to the flight crew.

Several performance monitoring systems and procedures of varying complexities (refs. 3–6) have been proposed over the years, but none have been implemented and tested on commercial transport aircraft. The Takeoff Performance Monitoring System (TOPMS) investigated in the current study was developed as a computer software and hardware graphics system to assist the pilot in the continual assessment of the takeoff situation. The TOPMS software drives cockpit displays that graphically indicate takeoff performance relative to a reference performance, engine condition, and a continually updated prediction of the runway position where the airplane can be braked to a stop if an aborted takeoff becomes necessary. It also provides explicit GO/NO-GO advice in the form of situation advisory flags (SAF's).

The TOPMS has been evaluated at the Langley Research Center in several phases. After a detailed TOPMS algorithm was formulated and developed in batch simulations (refs. 7 and 8), initial head-down display (HDD) graphics were implemented and evaluated on the Langley Transport Systems Research Vehicle (TSRV) real-time, fixed-base B-737 simulator. The TSRV is a highly modified Boeing 737-100 research airplane containing the research flight deck (aft) inside the fuselage. (See fig. 1.) Figure 2 is a photograph of the interior of the research flight deck; figure 3 is a close-up of the primary display (PD) navigational and TOPMS display (Nav/TOPMS), and the navigation control and display unit (NCDU).

The initial TOPMS displays were evaluated for content, credibility, and comprehensibility by 32 research, United States Air Force, airline, and industry pilots. They found that the displays were easy to monitor and provided valuable safety, performance, and advisory information currently unavailable in commercial cockpits. Additionally, the pilots suggested minor changes to the HDD graphics and recommended development of a simplified TOPMS head-up display (HUD) to complement the HDD. (See ref. 9.) A second simulation study followed that incorporated a revised HDD in front of each pilot and a simplified HUD in front of the Pilot Flying during takeoff. Seventeen evaluation pilots in the second study (including eight pilots who participated in the first study) provided additional insight into the desirability and importance of particular display symbology and formats. (See ref. 10.) Subsequently, the HDD graphics were revised further and the TOPMS was implemented on the TSRV research flight deck for the flight tests discussed in this report.

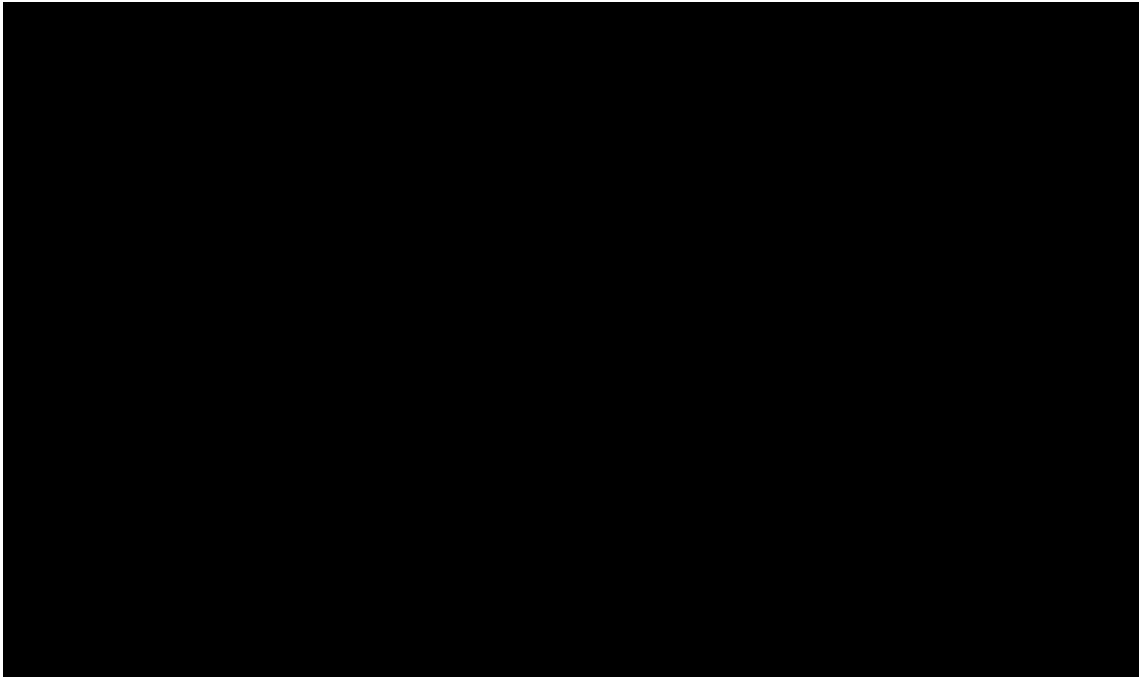
The TOPMS flight tests were focused on verifying that the TOPMS would operate satisfactorily in a

typically noisy airplane operating environment using preexisting flight computers, sensors, data buses, and displays. The TOPMS displays were available only to the pilot in the research flight deck (viz., the TOPMS Pilot) and only the latest version of the HDD symbology was tested. The test plan focused on producing appropriate displays for monitoring a variety of test conditions. Although most of the data gathered were qualitative, some numerical data were obtained during six test situations.

The remainder of this report contains a brief description of the TOPMS algorithm, a discussion of the TOPMS HDD symbology and format, photographs of the displays for various flight conditions, a description of the flight-test procedures and equipment, presentation and analysis of data (including pilot comments), and recommendations for further study.

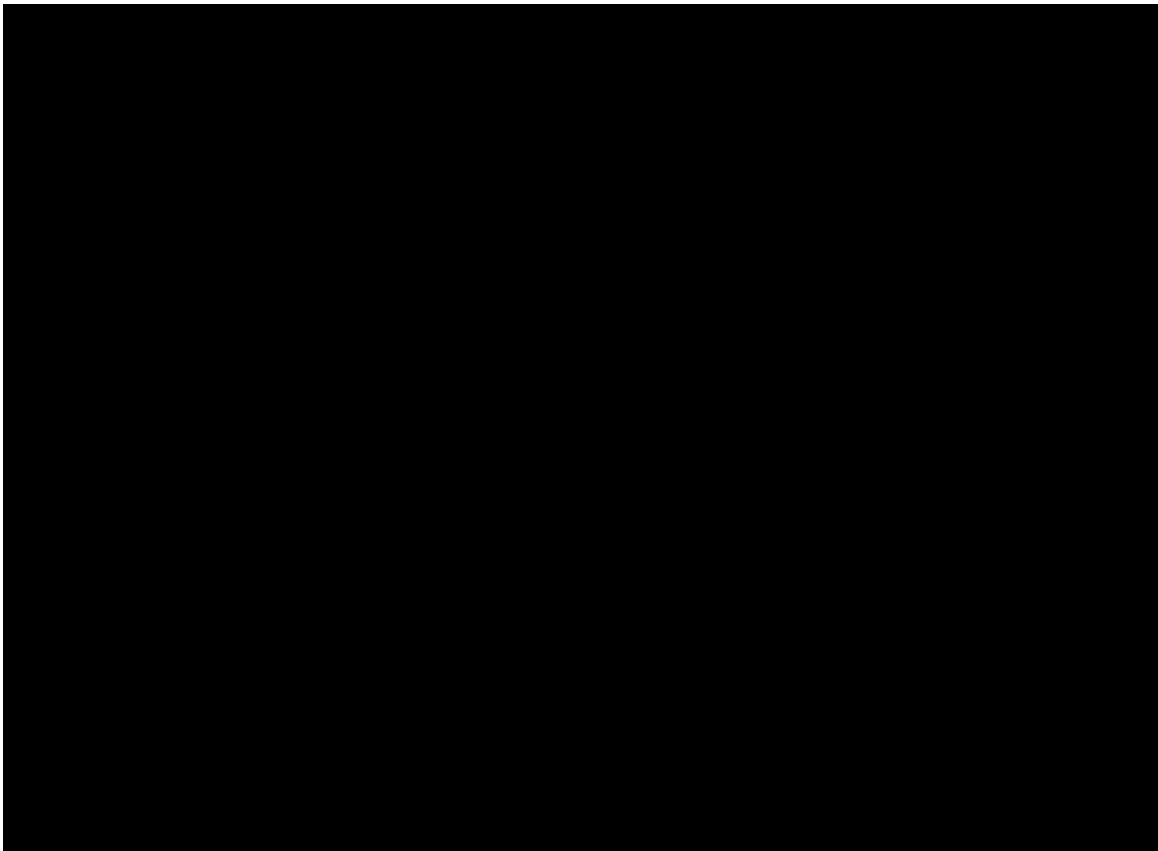
## Symbols

$A_n$	curve-fit coefficients, $n = 0, 1, 2, 3$ (eq. (2))
$a$	acceleration, ft/sec <sup>2</sup> (eqs. (1) and (2))
$D$	drag, lb
$d_a$	takeoff-roll computed distance from measured acceleration, ft
$d_{gs}$	takeoff-roll computed distance from measured ground speed, ft
$d_{lt}$	takeoff-roll measured distance from radar laser tracker, ft
$d_p$	takeoff-roll predicted distance from nominal acceleration, ft
$L$	lift, lb
$m$	mass, slugs
$n$	counter, consecutive error band excursions, $n = 5, 8, 10$
$T$	thrust, lb
$V_1$	critical engine safety CAS (decision speed), knots
$V_2$	takeoff safety CAS (climbout speed), knots
$V_R$	rotation CAS, knots
$V_T$	true airspeed, knots
$W$	airplane gross weight, lb
$\mu_r$	coefficient of rolling friction



L-80-2580

Figure 1. Cutaway view of TSRV B-737-100.



L-90-8320

Figure 2. TSRV research flight deck.

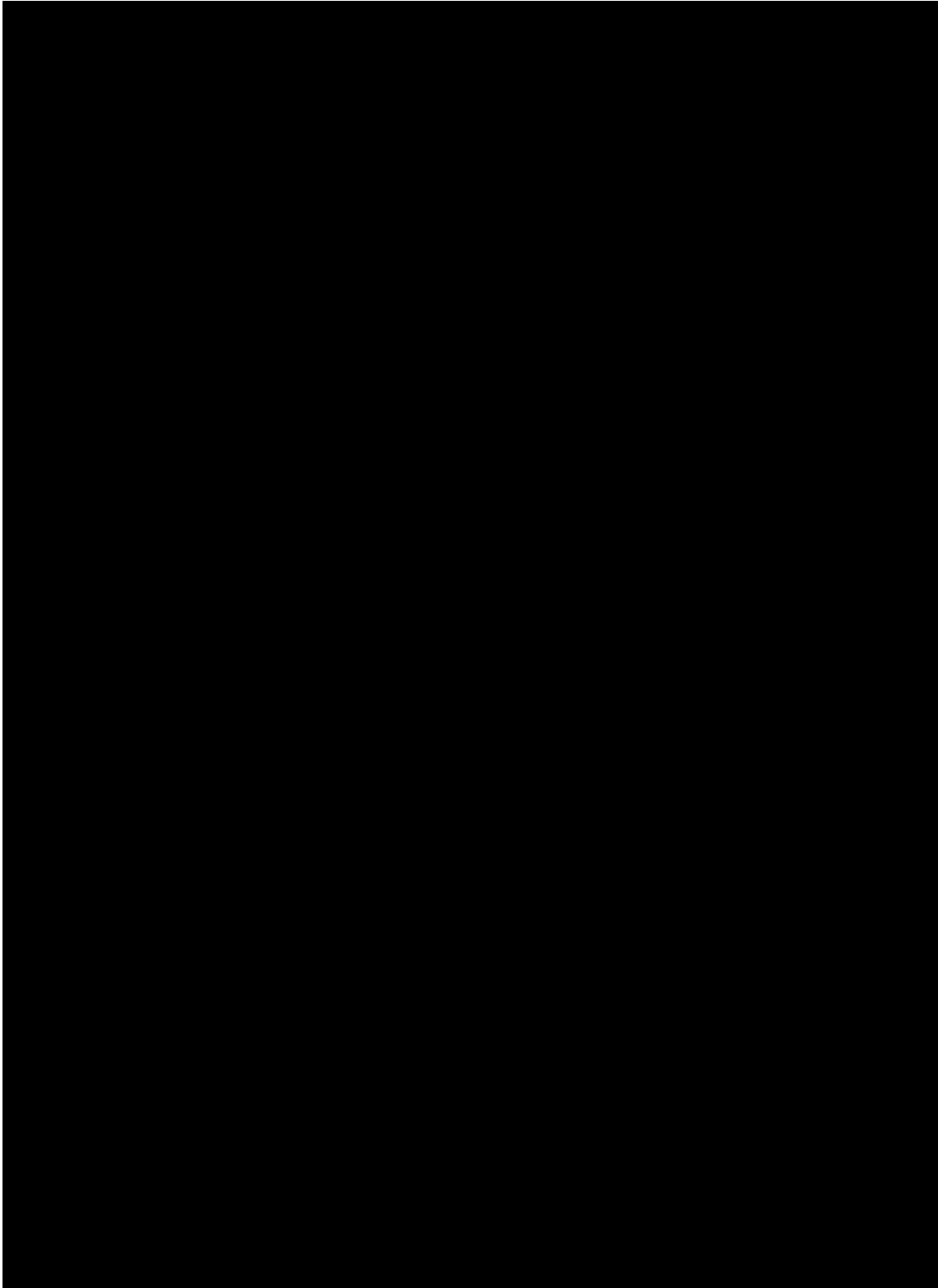


Figure 3. Displays in front of TOPMS Pilot.

L-90-08249

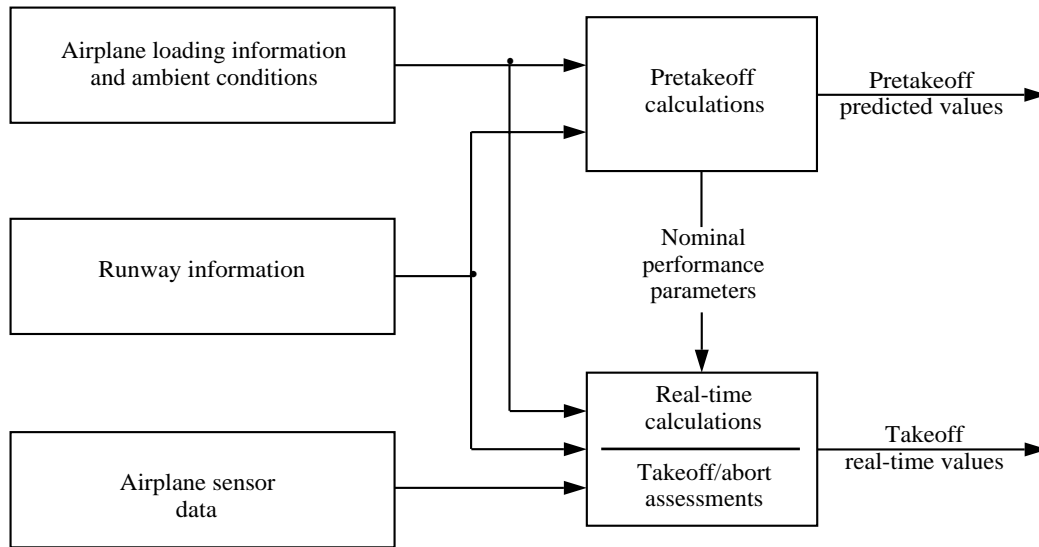


Figure 4. Functions of TOPMS algorithm.

#### Abbreviations:

accel.	acceleration
ADIRS	air-data and inertial reference system
CAS	calibrated airspeed, knots
DATA C	digital autonomous terminal access communication system
EASILY	Experimental Avionics System Integration Laboratory
EPR	engine pressure ratio
FAA	Federal Aviation Administration
GRLL	ground-roll limit line
HDD	head-down display
HUD	head-up display
IMU	inertial measuring unit
NCDU	navi gaton control and display unit
ND	navigation display
PD	primary display
SAF	situation advisory flag
TAS	true airspeed
TOPMS	Takeoff Performance Monitoring System
TSRV	Transport Systems Research Vehicle (B-737-100 class)

#### Description of TOPMS

The TOPMS is a computer software and hardware graphics system that visually displays engine status, runway performance, and situation advisory information to aid pilots with their GO/NO-GO decision to continue or to abort a takeoff. The TOPMS algorithm computes and manipulates airplane performance and related data and provides commands for the color display of both elemental and summary symbology. The elemental information consists of pretakeoff-predicted and real-time-measured indicators of performance and their effect on where the airplane is expected to reach takeoff speed or where it could be stopped in an abort situation (with maximum braking, but not reverse thrust). The summary information consists of situation-advisory flags (SAF's) that alert and advise the pilots when the takeoff situation has degraded to the degree that it may be wise to abort—or not to abort if insufficient runway distance is available for stopping the airplane on the runway pavement.

#### Algorithm

The TOPMS algorithm consists of two segments: a pretakeoff segment and a real-time segment as indicated by the block diagram in figure 4. The algorithm is briefly described in the next two sections; a detailed description of its development is given in references 7 and 8.

**Pretakeoff calculations.** When activated during pretakeoff, the algorithm obtains and uses nominal and/or current values for several key parameters (table I); checks for system anomalies such as



misconfigured flaps or inconsistent input data; and determines scheduled values for engine pressure ratio (EPR), critical engine safety speed  $V_1$  (also called decision speed), rotation speed  $V_R$ , and takeoff safety speed  $V_2$ . The algorithm extracts values for these parameters from data files that contain pertinent tables from the airplane flight manual.

Table I. Pretakeoff Inputs  
to TOPMS Algorithm

Airplane center of gravity
Airplane gross weight
Airplane flap setting
Pressure altitude
Wind direction
Wind speed
Ambient temperature
Runway rolling friction coefficient

Using data from detailed mathematical models of the engines, landing gear, and aerodynamics for the host airplane, nominal values for the parameters listed in table I, and the appropriate EPR value for existing conditions, the algorithm calculates a predicted nominal acceleration performance of the airplane for the planned takeoff. It also predicts where  $V_1$  and  $V_R$  should occur during a nominal takeoff roll and warns the pilot when the length of the assigned runway appears too short for the planned takeoff.

The nominal performance is represented by a curve of nominal acceleration versus true airspeed  $V_T$  generated from equations (1) and (2) and plotted with an appropriate curve-fitting method. Equation (1) defines the nominal acceleration during the takeoff roll as

$$a = \frac{T - D - \mu_r(W - L)}{m} \quad (1)$$

where the airplane approximate gross weight  $W$  is known, the rolling-friction coefficient  $\mu_r$  is estimated for the perceived runway surface condition, the values of lift  $L$  and drag  $D$  are obtained by the algorithm from the aerodynamics mathematical model, and thrust  $T$  is computed from the engine model for a typical throttle-movement history from idle to the position of scheduled EPR.

The same acceleration as a cubic polynomial in  $V_T$  which is fitted to the equation (1) curve through the coefficients  $A_n$  of the powers of  $V_T$  (where  $n = 0, 1, 2, 3$ ) is expressed as

$$a = A_0 + A_1V_T + A_2V_T^2 + A_3V_T^3 \quad (2)$$

The conversion process involves the following steps:

1. Equation (1) is solved using an extremely low value of  $\mu_r = 0.005$  and nominal values for other conditions over the takeoff speed range. The resulting curve (after engine spool-up transients settle out) is plotted as the upper boundary in figure 5 over a speed range from approximately 10 knots to  $V_R$  speed.
2. Equation (1) is solved again for an extremely high value of  $\mu_r = 0.04$  and plotted as the lower boundary in figure 5 over the same speed range.
3. Equation (2) is fitted to each of the above curves using the sum of least-squares error method. As shown in figure 5, the correlation using this method is excellent (the computed and fitted curves for each value of  $\mu_r$  essentially lie on top of each other).
4. The two sets of curve-fit coefficients are then stored where the algorithm can access them when subsequently creating a nominal acceleration curve corresponding to any estimated value of  $\mu_r = 0.005$  to  $0.040$ .

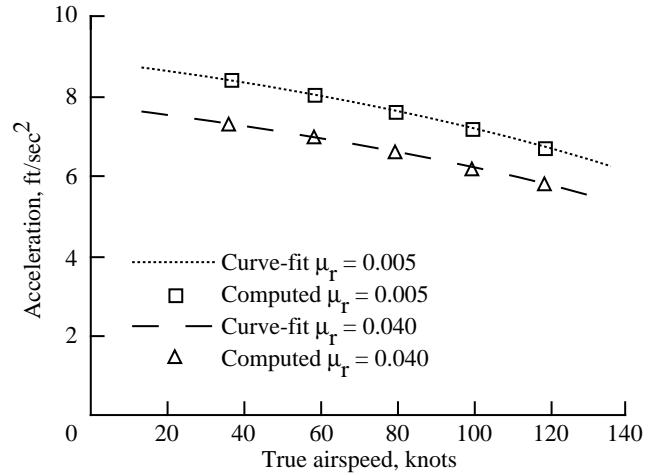


Figure 5. Acceleration curves for extreme values of  $\mu_r$ .

A representative nominal acceleration curve for a dry surface ( $\mu_r = 0.015$ ) is plotted as a solid line in figure 6. This curve is created by linear interpolation of the two sets of curve-fit coefficients obtained above. After the curve-fitting process is complete, the pre-takeoff segment nominal performance parameters are transferred to the real-time segment, as shown in figure 4. This process is treated in considerable detail in reference 8.

**Real-time calculations.** A block diagram portraying real-time operations is shown in figure 7.

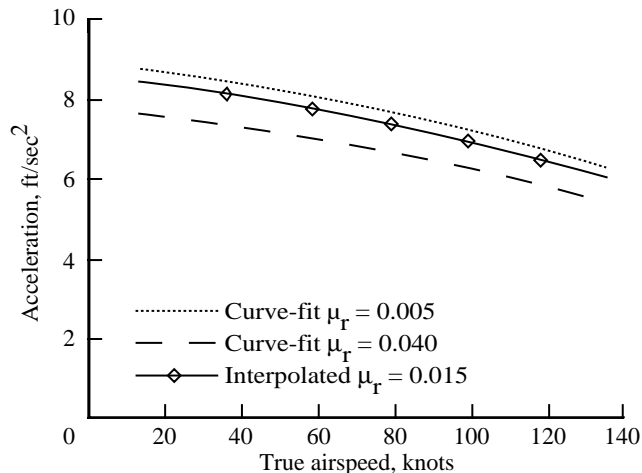


Figure 6. Nominal acceleration for dry runway surface.  
 $\mu_r = 0.015$ .

The functions performed by most of the blocks are self-explanatory; the measured inputs enter from the left and the computer-estimated outputs emerge at the right. At low speeds, the algorithm uses measured ground speed and wind to compute airspeed; then at approximately 40 knots, the airplane real-time-computed airspeed becomes valid and replaces airspeed derived from integrated ground speed by

means of the software switch shown at the left center of figure 7. During the test runs, airplane positions on the runway were determined from distances traveled calculated by double integration of measured accelerations (method 1). During postflight analysis (only), single integration of the independently measured ground speed provided another means of determining airplane position (method 2 is shown by the dashed line at the top of fig. 7).

The real-time segment of the algorithm is activated when the pilot advances the throttles forward from idle. As the airplane rolls down the runway, the distance traveled and the distances required to reach  $V_1$  and  $V_R$  are continually computed using sensor-measured values for the parameters shown in table II.

Table II. Additional Real-Time Inputs to TOPMS Algorithm

Left and right engine pressure ratios  
Left and right throttle positions  
Airplane flap settings  
Airplane accelerations  
Airplane ground speed  
Calibrated airspeed

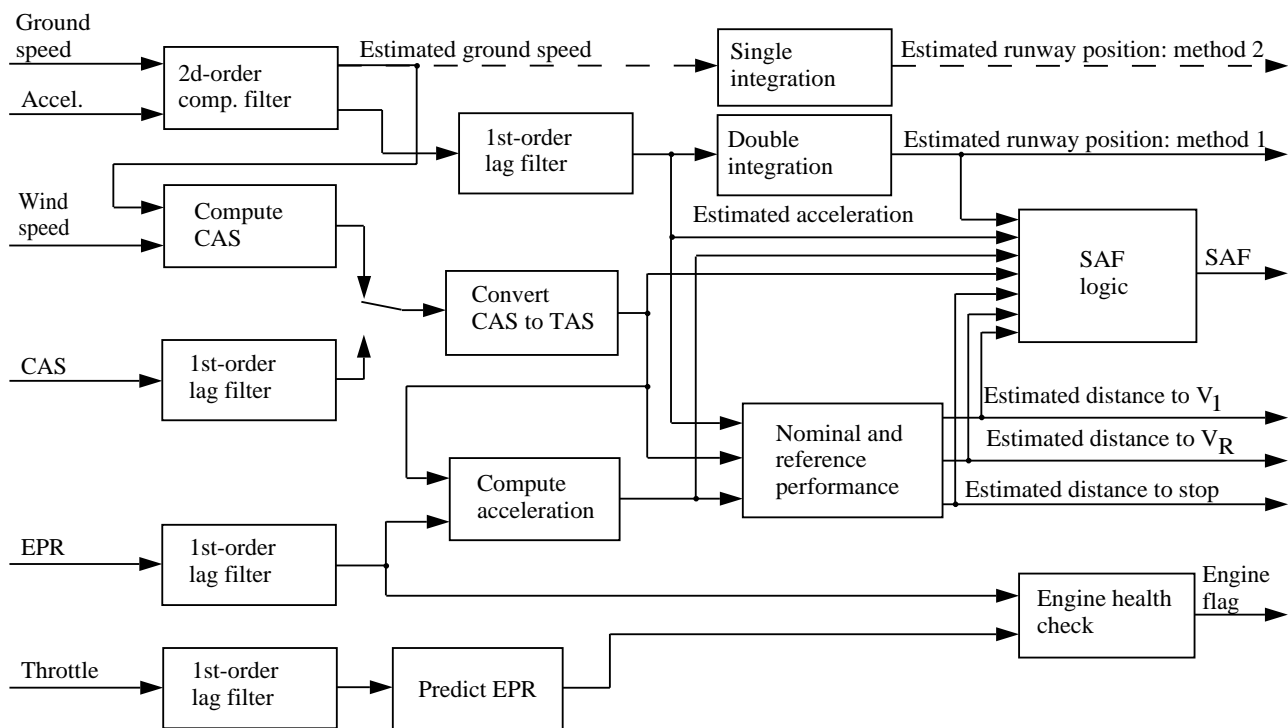


Figure 7. Algorithm real-time functions.

The algorithm also creates a reference acceleration curve in real time in the following manner:

1. While the throttles are being advanced and/or adjusted, a reference acceleration is computed from equation (1) using thrust values associated with the sensed EPR and otherwise nominal input data.
2. As soon as the throttles are set (i.e., become stationary for more than 3 sec), the algorithm makes a one-time  $\mu_r$  adjustment to the reference acceleration curve by forcing the reference acceleration value at a given true airspeed to match that of the measured acceleration. This adjustment is achieved by appropriately changing the value of  $A_0$  in equation (2).
3. The algorithm also makes a one-time adjustment to the along-track component of the wind. After the calibrated airspeed CAS measurement becomes valid, an along-track component of the wind is calculated from measured ground speed and CAS; this value is then substituted for the initial value for the remainder of the takeoff.

As indicated above, the  $\mu_r$ - and wind-error adjustments are programmed to execute only once per run. However, each time the throttles are moved appreciably, the algorithm adjusts the reference acceleration curve according to the EPR levels it associates with each newly measured throttle position.

Throttle movements and settings that differ from those assumed when the nominal acceleration curve was created are not treated by the TOPMS algorithm as error conditions; instead, they produce a reference acceleration curve that is parallel to the nominal acceleration curve. In particular, during a low-throttle takeoff, the displays will not indicate an engine problem and SAF's will not appear if the remaining runway distance will accommodate the extended takeoff. The algorithm could be rewritten to treat off-nominal throttle settings as an error; but because such an error is easily corrected by moving the throttles, low-throttle settings probably should not be included in the abort criteria.

The algorithm real-time segment continually computes the difference between measured acceleration and reference acceleration. If the magnitude of the resulting error signal exceeds a specified level, an abort SAF is displayed. (Refer to "Data Analysis and Results" for additional comments.)

### Display Format and Symbology

Figure 3 is a close-up of the displays in the TSRV aft research flight deck. The upper primary display

(PD) screen provides attitude, altitude, and speed information. The existing PD system configuration was used without modification for the TOPMS tests. The navigation display (ND) in the center of the photograph presents either TOPMS information while the airplane is on the ground or regular navigational information after the airplane becomes airborne. The keypad on the unit below the ND screen is used to enter data into the airplane computers.

The TOPMS display consists of a runway graphic with passive and active symbology on and around it. Figure 8 illustrates the display for two situations: the takeoff-roll display (fig. 8(a)) shows a takeoff roll under way in which acceleration performance has become unsatisfactory and an abort is being advised and the abort display (fig. 8(b)) shows a takeoff roll in which an abort has been initiated and partial braking is under way.

The takeoff-roll situation illustrated in figure 8(a) shows the airplane about halfway down a 6000-ft runway traveling at a CAS of 97 knots (displayed in the box left of the airplane symbol). Pretakeoff computations for this case were based on nominal acceleration and the algorithm predicted that a decision speed  $V_1$  of 126 knots and a rotation speed  $V_R$  of 128 knots could be achieved near the unshaded triangle. However, during the takeoff roll, actual acceleration was considerably below nominal, which caused the horizontal  $V_1$  and  $V_R$  lines and the shaded triangle to move forward. Specifically, the position of the  $V_R$  line corresponds to the computed along-track position of the shaded triangle apex. This forward movement of the shaded triangle is an indirect but, nevertheless, an important indication of the acceleration deficiency.

The algorithm initially determines whether a Federal Aviation Administration (FAA) sanctioned takeoff (ref. 11) can be expected; it computes whether the airplane can achieve  $V_R$  before it reaches the ground-roll limit line (GRLL). The GRLL marks the furthestmost downfield position where the airplane, after undergoing a critical engine failure at  $V_1$ , can initiate rotation and barely clear a 35-ft barrier at the end of the runway. The minimum takeoff field length is the total distance required to reach  $V_R$  plus the ground and air distance beyond  $V_R$  for completing the takeoff described above.

For the situation illustrated in figure 8(a), the ground and air distance beyond  $V_R$  is subtracted from total runway length (6000 ft) to establish the location of the GRLL. Note that a takeoff-roll safety margin of approximately 500 ft is evident between the apex of the shaded triangle (viz., the  $V_R$  line) and the

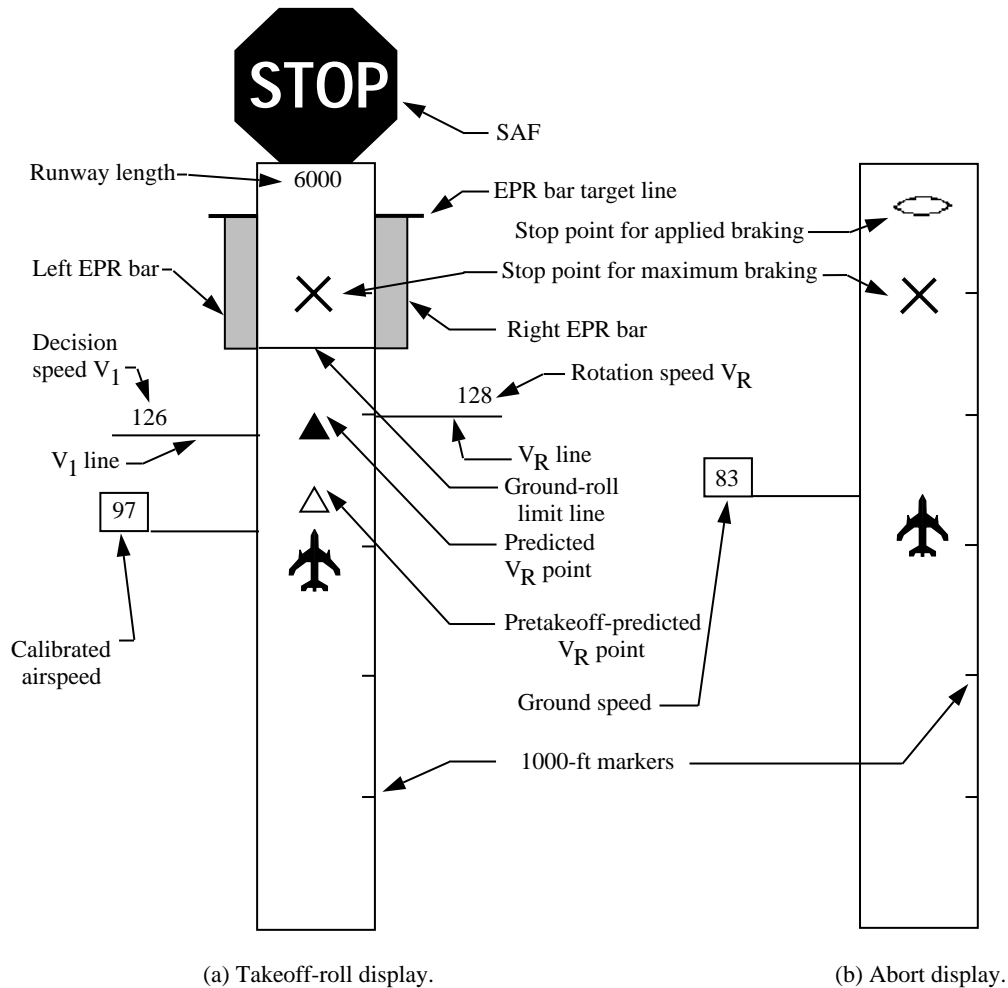


Figure 8. TOPMS takeoff-roll and abort-display symbology.

GRLL. The GRLL has no direct relationship to the bottom of the EPR bars; they were arbitrarily based at the GRLL on the display format.

In the off-nominal situation depicted in figure 8(a), both engines appear to be operating normally. The EPR bars are extended up to the target level, but the shaded triangle and the  $V_1$  and  $V_R$  lines have moved noticeably forward from their nominal locations depicted by the unshaded triangle. The algorithm has determined that an abort may be the most appropriate control action for this situation and the display conveys this advice to the pilot by means of the STOP SAF that appears at the end of the runway graphic. At the same time, an  $\times$  appears just beyond the GRLL and shows where the airplane will come to a stop with maximum application of the wheel brakes and full deployment of the spoilers (i.e., speed brakes). Normally, the  $\times$  remains hidden until the computed stop point is beyond the GRLL; when an abort is advised, the  $\times$  is unmasked simultaneously

with the appearance of the STOP sign. The benefit of using reverse thrust is not included in the calculation of the  $\times$  position; however, reverse thrust can be used to advantage in situations where both engines appear to be working satisfactorily. (See fig. 8.)

Figure 8(b) shows the TOPMS display after an abort has been initiated. All takeoff-related information has been removed from the runway graphic except the airplane symbol, which shows position on the runway; ground speed, which replaces CAS in the speed box; and the  $\times$ , which locates the maximum-braking stop point. An additional symbol, shaped like a football, has appeared that denotes the predicted stop point based on the measured acceleration. Less than maximum braking is required whenever the football position is ahead of the  $\times$ .

### Summary of Situation Advisory Flags

A summary of SAF responses based on sensor data during various flight situations is shown in

Table III. Shapes, Colors, and Conditions for the SAF's

SAF shape	SAF color	Flight situation (sensor input)	Advisory
No flag		1. Takeoff roll proceeding satisfactorily	GO
Rectangular	Green	2. No engines failed; airplane can attain $V_R$ before reaching GRLL but stopping on runway doubtful	GO
		3. One engine failed when $CAS > V_1$ ; airplane can attain $V_R$ before reaching GRLL but stopping on runway doubtful	GO
Triangular	Amber (blinking)	4. One engine failed at $CAS > V_1$ ; airplane can attain $V_R$ well before reaching GRLL or can easily stop on runway	EITHER
Octagonal	Red	5. One engine failed at $CAS < V_1$	NO-GO
		6. Both engines failed	NO-GO
		7. Predicted rotation point beyond GRLL	NO-GO
		8. Measured along-track acceleration not within the specified error band about the reference acceleration	NO-GO

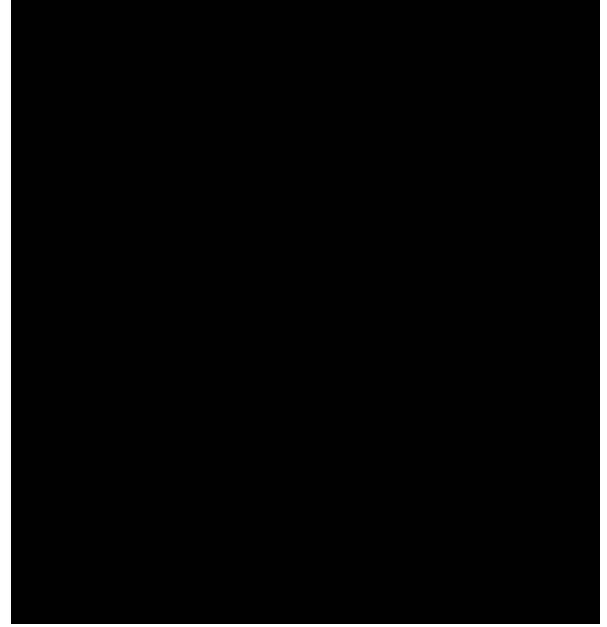
table III. The absence of an SAF indicates that the takeoff is proceeding normally and/or airplane parameters are staying within acceptable error bands. Flight situation 4 informed the pilot at a critical high-speed point that an engine had failed and that adequate runway distance remains to stop the airplane if the GO option suddenly became unreasonable (e.g., when smoke is rapidly engulfing the cabin).

### Displays for Several Takeoff and Abort Situations

No still photographs of the displays were made during actual flight tests. Instead, all photographs except those in figures 1, 2, and 3 were recreated in a Langley special-purpose test facility, the Experimental Avionics System Integration Laboratory (EASILY). In essence, EASILY is a hot-bench extension of the flight test bed. It contains duplicates of the actual flight hardware and software along with a high-fidelity, nonlinear computer model of the Boeing 737-100—the same model as the TRSV used during the TOPMS simulation studies. (See refs. 9 and 10.)

#### Pretakeoff Displays

If the positions of the flaps do not agree with the nominal position specified for the pretakeoff calculations, the partially generated TOPMS display shown in figure 9 will appear on the screen. No additional TOPMS graphics are generated until the flap lever is put in the proper detent and the flaps move to the commanded position.

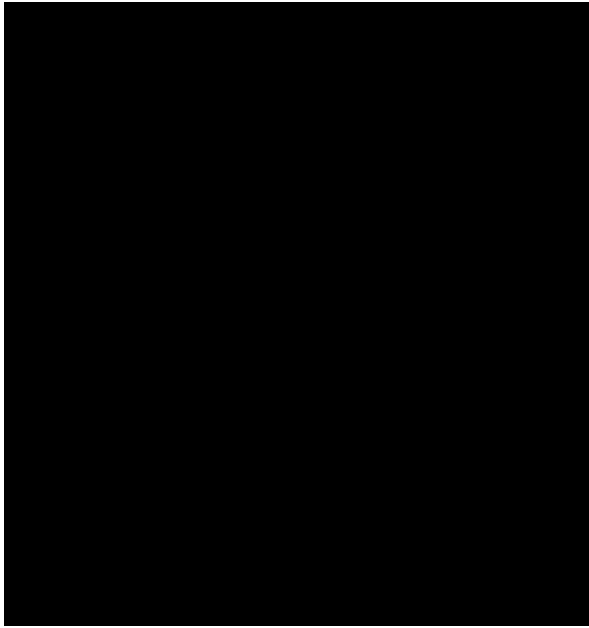


L-92-02984

Figure 9. TOPMS display with flaps in wrong position.

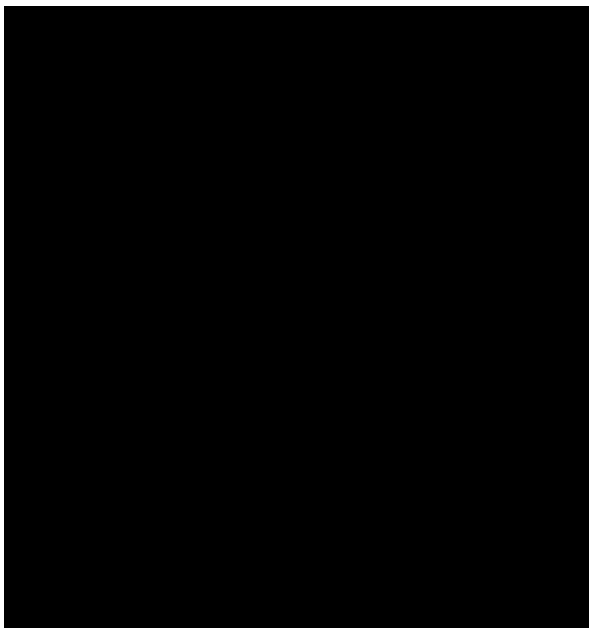
If the length of the assigned runway is shorter than the minimum distance determined by the algorithm, a TOPMS display similar to the one in figure 10 will appear. Note that the apex of the  $V_R$  triangle is well beyond the GRLL (horizontal line across the runway symbol), which causes a STOP sign to appear that advises the pilot not to start the takeoff roll.

If the runway length is long enough, the flaps are correctly set, and the conditions are otherwise normal, a fully generated pretakeoff TOPMS display



L-92-02985

Figure 10. TOPMS display when assigned runway too short.



L-92-02986

Figure 11. TOPMS display when ready to begin takeoff.

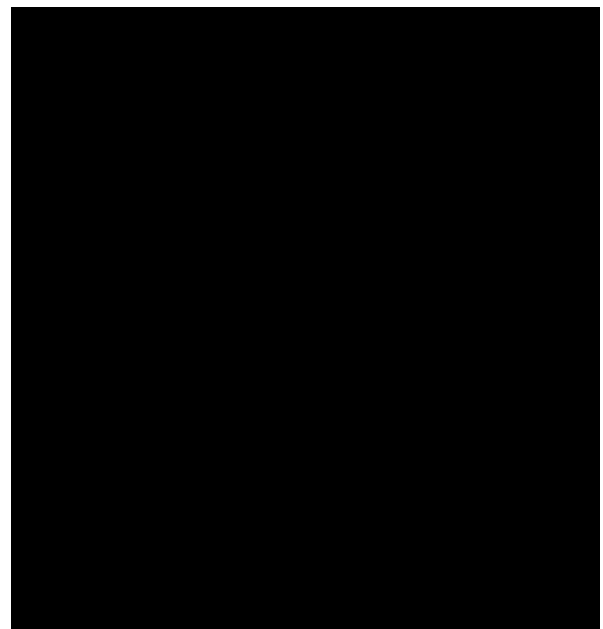
similar to the graphic shown in figure 11 will appear. This graphic shows where  $V_1$  of 122 knots and  $V_R$  of 124 knots should occur with respect to the airplane initial position on the runway. (For viewing clarity, the computed airplane position is depicted by the nose of the airplane graphic.) The length of the assigned runway (6000 ft) and the point where the takeoff roll will start have been entered; the algorithm has scaled the corresponding runway graphic

to span the entire usable vertical range of the display screen. At this stage, the TOPMS is ready for the takeoff roll to begin. (The zero-length EPR bars depicting idle thrust are not perceptible in fig. 11.)

### Takeoff-Roll Displays

Photographs of representative displays for several flight situations are presented in figures 12–19.

**Normal takeoff roll.** Figure 12 shows a typical TOPMS display during a normal takeoff roll on a 6000-ft-long runway. The airplane is traveling at a CAS of 83 knots. Note that the top ends of both EPR bars match their target levels (1.95) and that the  $V_R$  triangles have not separated. Under such conditions, the pilot can expect to reach  $V_R$  approximately halfway down the runway and the monitoring tasks would primarily be to keep track of airspeed and occasionally to glance at the  $V_R$  triangle and EPR bars. The pilot can monitor airspeed by watching the numerals in the speed box or by observing the closure of the moving CAS line on the near-stationary  $V_1$  line. The pilot can also keep the analog display of airspeed within peripheral vision range while continuing to focus on the real-world runway scene.



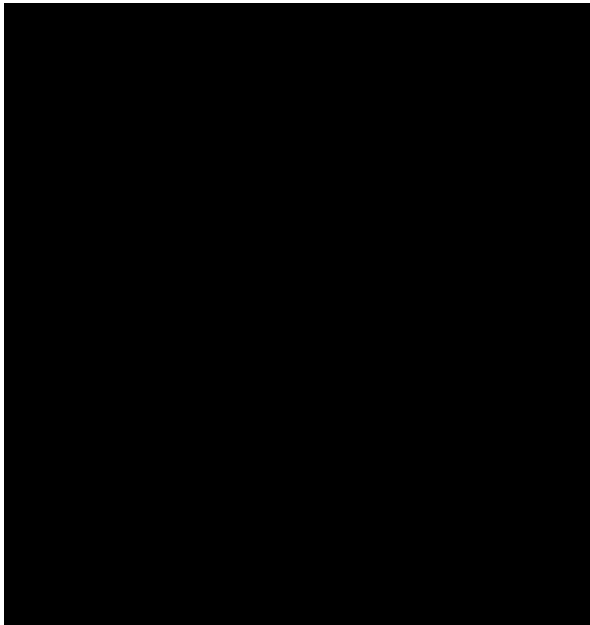
L-92-02987

Figure 12. TOPMS display when normal takeoff under way.

If an engine were to fail before the airplane reaches  $V_1$  (during an otherwise normal takeoff situation), it would produce a head-down TOPMS display similar to the one shown in figure 3. In this instance, the right engine has failed at approximately 100 knots and the display is conveying an abort SAF

(STOP sign) to the pilot. Additionally, the algorithm has determined that for an immediate abort and use of maximum braking, the airplane can be stopped at the  $\times$  shown about halfway down the 6000-ft runway.

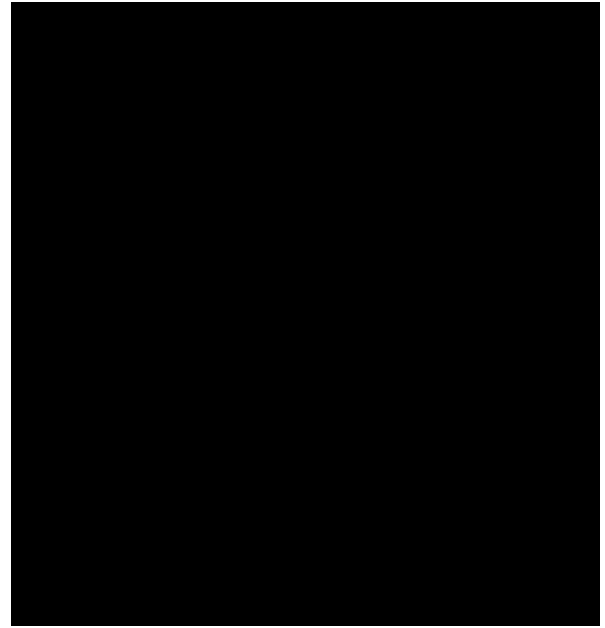
**Low-throttle takeoff roll.** Figure 13 shows the TOPMS display for a situation in which the throttles were not advanced to the nominal position for attaining scheduled EPR (selected during pretakeoff by the algorithm from the database programmed from the TSRV flight manual). The shaded triangle has moved forward nearly 1000 ft from its initial location where it had been superimposed on the unshaded triangle. If the shaded triangle remains stationary at this new position, it signifies that thrust is correct for the actual throttle setting and no acceleration error exists. The throttles can be advanced to reduce this separation or the takeoff roll can be continued at reduced thrust with the expectation of a satisfactory takeoff. In alternate form, the algorithm could respond to the low-throttle settings with error condition graphics; this was not the choice in any of the TOPMS studies. (See refs. 7–10 and 12.)



L-92-02997

Figure 13. TOPMS display with throttle set lower than scheduled.

**Engine failure during low-throttle takeoff roll.** If an engine fails during a reduced-thrust takeoff-roll situation, the TOPMS display will be similar to the graphic shown in figure 14. An engine failure is declared by the algorithm when the engine EPR has degraded by more than a specified amount (10 percent in this study) from the value normally

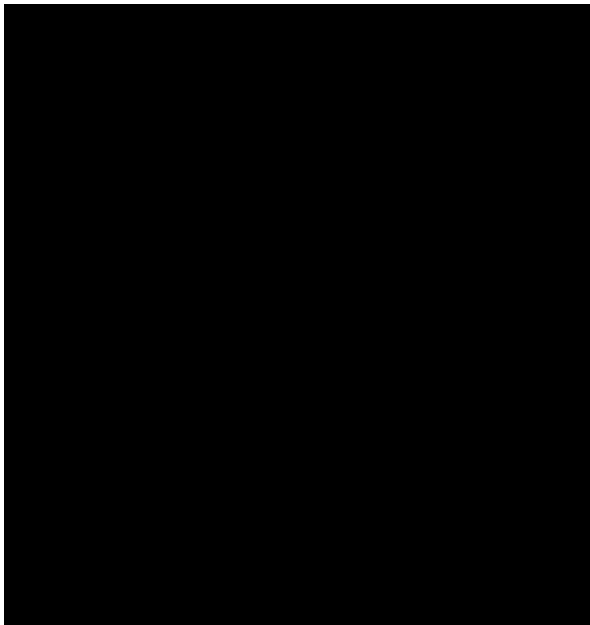


L-92-03001

Figure 14. TOPMS display for engine failure during reduced-throttle takeoff.

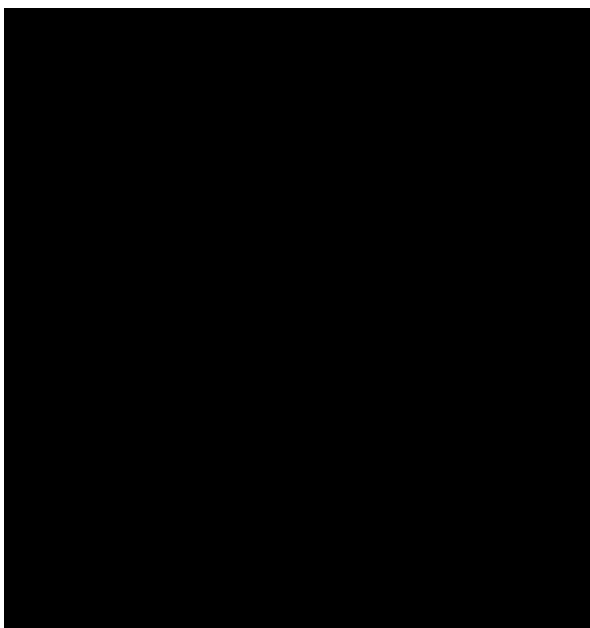
produced for the measured throttle position. For the situation in figure 14, the under-advanced throttles are commanding both engines to produce EPR's of approximately 1.7 rather than the scheduled 1.95. The left engine is apparently producing the commanded EPR value of 1.7; however, the EPR bar for the failed right engine is clearly less than 90 percent of the length of the apparently correct left EPR bar and has turned red. Concurrently, a red SAF (STOP sign) and a predicted stop point  $\times$  have appeared and the  $V_R$  triangles have separated by more than 1000 ft. If the performance of the faulty engine degrades further, the shaded triangle will continue to advance toward the GRL. At this stage, takeoff is still a viable option; however, NO-GO is the control action recommended by the TOPMS before airplane speed increases further and the remaining runway distance becomes more marginal.

**Engine failure at high speed.** If an engine failure occurs near  $V_1$  on a relatively short runway, as shown in figure 15, the SAF is displayed as a large green rectangle at the end of the runway graphic. This symbol advises the pilot that the best option is to continue with the takeoff because a maximum-braking stop would likely terminate near or beyond the end of the runway pavement. (See the  $\times$  in fig. 15.) Also, note in figure 15 that the current CAS = 124 knots is greater than the decision speed  $V_1 = 120$  knots, which is an overriding condition that warrants continuation of the takeoff.



L-92-03000

Figure 15. TOPMS display for engine failure near  $V_1$  on short runway.



L-92-02996

Figure 16. TOPMS display for engine failure after reaching  $V_1$  on very long runway.

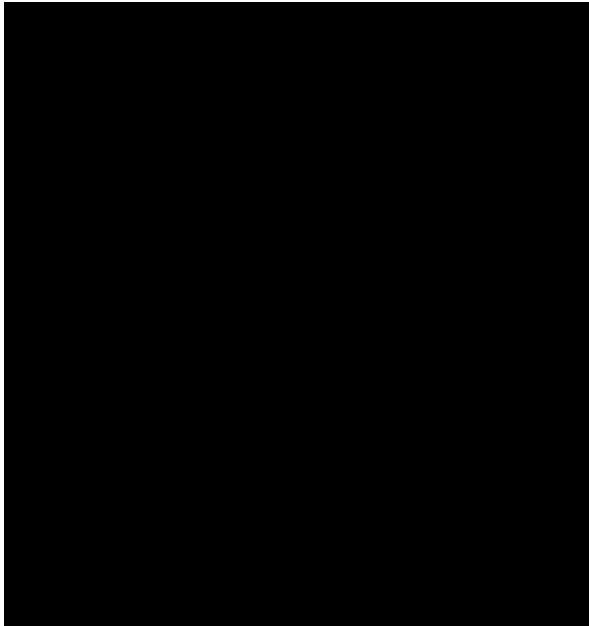
If a similar situation were encountered on a very long runway, the TOPMS would exhibit a blinking triangular GO/NO-GO SAF like the one shown in figure 16. The blinking amber SAF signifies that an engine has failed at or above  $V_1$  and that the two viable control options include continuing the takeoff as currently required by regulations (ref. 11)

or undertaking a dangerous high-speed abort (e.g., in a perceived critical emergency such as fire or smoke in the cabin). For the situation in figure 16, the predicted maximum-braking stop point  $x$  is about 6000 ft down the 10 000-ft runway.

**Excess drag versus EPR sensor error.** Ascertaining whether excessive drag and/or large EPR sensor errors are causing significantly lower than nominal performance involves the following condition checks by the algorithm:

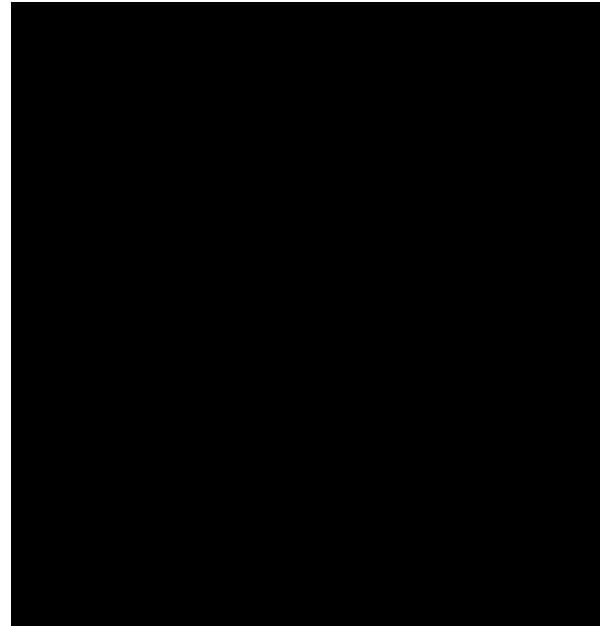
1. Engine performance is checked. A failing engine produces lower than scheduled EPR and a correspondingly lower acceleration level. When the EPR error for this engine becomes unacceptable (i.e., the measured EPR level differs by more than 10 percent from the EPR level associated with the measured throttle position), the algorithm changes the color of the shortened EPR bar to red and displays the appropriate SAF. (See fig. 3.) If the pilot chooses not to abort immediately, the algorithm will continue to provide information on the magnitude and trend of the acceleration deficiency by the position and movement of the shaded triangle and on the EPR condition of the unfailed engine by the length and color of its associated EPR bar.
2. If no engine has failed and the throttles have a lower than nominal setting (fig. 13), the EPR bars will accordingly stop short of their target mark, but they will not change color. The shaded triangle will also move noticeably forward; no SAF will be displayed unless the triangle moves beyond the GRLL.
3. If the EPR bars rise to and remain at their scheduled target level without changing color and the shaded triangle continually drifts forward, the indication is that drag is increasing faster than it should for the other conditions (i.e., wind, temperature, weight, etc.). The situation is illustrated in figure 17. When the incremental drag becomes excessive, causing the acceleration error to exceed the acceptable level of 10 percent, a red SAF (STOP sign) will appear as shown in figure 18. However, if one or both EPR bars turn red while remaining at the target length, a serious EPR sensor error exists and a red SAF will appear as shown in figure 19. Note in this figure that the shaded triangle has also crossed the GRLL, thus satisfying another abort criterion (situation 7 in table IV). A relevant, real-world situation that resulted from an EPR sensor error is discussed in a later section of this report.





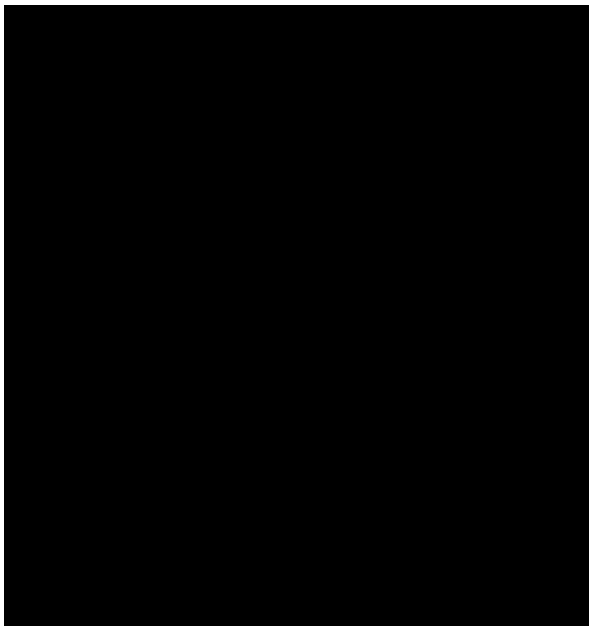
L-92-02994

Figure 17. TOPMS display with acceptable acceleration deficiency.



L-91-15892

Figure 19. TOPMS display with serious disagreement between indicated and measured EPR's.



L-92-02988

Figure 18. TOPMS display with unacceptable acceleration performance.

### Abort Displays

Figure 20 shows photographs of abort displays for three situations. Each display contains two computer-predicted stop point symbols—the  $\times$  that is carried over from the takeoff display and the football-shaped symbol that appears on the runway

graphic as soon as the brakes are applied. The football locates where the stop point will be based on the currently computed position, speed, and measured acceleration. The display in figure 20(a) shows the football ahead of the  $\times$ , which indicates that less than full braking is being applied. The display in figure 20(b) shows the football superimposed on the  $\times$ , which indicates that full braking is being applied. The display in figure 20(c) indicates that full braking and reverse thrust are being applied to stop the airplane slightly before the  $\times$  is reached.

### Test Equipment

The TSRV is a production prototype Boeing 737-100 airplane (fig. 1) with its fuselage filled with numerous computers, recorders, data-transfer systems, and the aft research flight deck that permit the use and evaluation of advanced electronic displays and fly-by-wire controls. A TOPMS display was not provided in the TSRV forward regular flight deck; brake controls and HUD were not provided in the research flight deck. Because of these equipment limitations, the TOPMS was remotely tested in the HDD mode only.

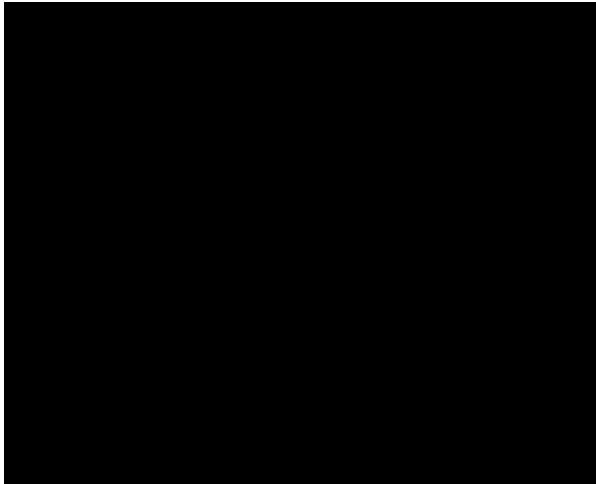
A functional block diagram of the test hardware is shown in figure 21. Although the TOPMS Pilot and TOPMS displays were located remotely, the procedures were set up to simulate a side-by-side, real-world piloting situation. The TOPMS Pilot and the Pilot Flying communicated by intercom.

Table IV. Number of Runs at Various Test Situations

Test situation <sup>a</sup>	Runs with IMU used on test day—			Runs with ADIRS used on test day—	Runs with body-mounted accelerometer used on test day—			Total runs
	1	2	3	4A	4B	5	6	
Takeoffs								
1. Normal	4	3	3	5	5	4	2	26
2. Low-thrust setting	1	2	4	1	2	3		13
3. Low, then normal thrust		1	1		3	1		6
4. Large $\mu_r$ -error correction	1	2					2	5
5. Large wind-error correction	2	2					1	5
Aborts								
6. Intentional	1	1					1	3
7. Unacceptable acceleration deficiency		1	4		2	2	1	10
8. Simulated engine failure	1	3	7		1	3	2	17
Totals	10	15	19	6	13	13	9	85

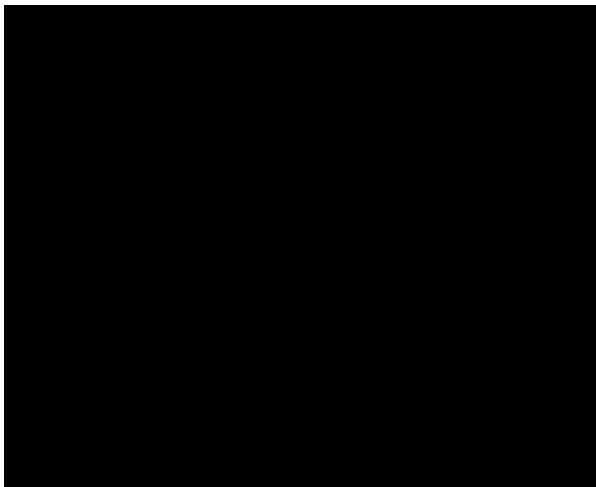
<sup>a</sup>Test situations

1. In addition to normal takeoffs at the test sites, data were obtained for all takeoffs going to and returning from these sites; consequently, approximately 30 percent of the runs listed in Table IV were normal takeoffs.
2. Low-thrust takeoffs were made with EPR settings of 1.6 and 1.7 rather than the nominal EPR settings of 1.88 to 1.95.
3. These runs were begun with significantly lower than nominal throttle settings; during the takeoff roll, the Pilot Flying deliberately moved the throttles up and down several times so the TOPMS Pilot could observe the response of the shaded triangle as it continually updated the position for reaching  $V_R$ .
- 4, 5. One-time adjustments to  $\mu_r$  and the head wind were automatically made (if necessary) on all runs. However, to make this feature noticeable to the TOPMS Pilot, intentionally large  $\mu_r$  and wind errors were manually entered for several pretakeoff computations. Subsequent throttle adjustments translated to the display as small movements of the shaded triangle each time the throttles were reset and remained stationary for more than 3 sec.
6. Three runs were intentionally aborted and the airplane was stopped with maximum-braking application; the laser tracker at the Wallops Flight Facility tracked the airplane during two of the stops.
7. Ten takeoff rolls were made with the spoilers fully deployed to create excess drag as airplane speed increased. In response, the shaded triangle was observed to creep forward until the resulting acceleration error tripped the abort SAF. (See fig. 18.)
8. Engine failures were simulated when the Safety Pilot appropriately moved one throttle to artificially induce an EPR discrepancy. For this test only, the algorithm compared the EPR value associated with the current deflected throttle position and its initial target value. Such failures were detected by the TOPMS Pilot as a shrinking red EPR bar and an accompanying abort SAF. (See fig. 3.)



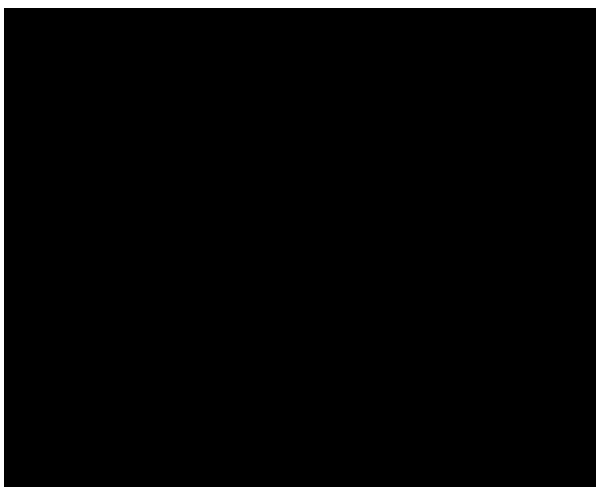
L-92-02989

(a) Partial braking.



L-92-02991

(b) Full braking, except no reverse thrust.



L-92-02992

(c) Full braking, including reverse thrust.

Figure 20. TOPMS displays for three braking levels.

The TOPMS software was programmed on the Norden 11/70 displays computer console (fig. 1) along with the software for the other airplane displays. Except for a video camera and an additional remote display screen, no extra hardware had to be installed to document the real-time performance of the TOPMS displays under the various test situations. Research observations and conversations among the pilots, the flight director, and the control tower were recorded on the audio channel of the videotapes.

The TOPMS interfaced with the flight decks, sensors, and other experimental equipment through the airplane global digital autonomous terminal access communication (DATAC) data bus. (See ref. 13.) In addition, a ground-based FPS-16 Radar/Laser Tracker (ref. 14) at the Wallops Flight Facility was used to track the airplane during several of the test runs; it independently provided distance measurements as functions of time. Subsequently, these data were time merged with the data recorded onboard the airplane, which permitted a comparison of measured and computed stop distances. Sixteen channels of strip-chart data were monitored during the test runs to verify in real time that a test run appeared to be proceeding properly. In addition, approximately 60 airplane and TOPMS parameters were digitally recorded at a rate of 20 samples per second for postflight scrutiny and analysis.

## Description of Flight Tests

Six days of flight testing were conducted between March 1987 and November 1989 at the Wallops Flight Facility and the Langley Air Force Base in Virginia, the Kennedy Space Center Shuttle Landing Facility and the Patrick Air Force Base in Florida, and the Asheville Regional Airport in North Carolina. The test runs included 55 takeoff and 30 abort situations. All were made on dry pavements ranging from slurry-sealed asphalt to highly grooved concrete. During the test series, temperatures ranged from approximately 25° to 85°F and gross weights varied from heavy to light depending on the amount of fuel onboard.

## Flight Test Crew

As indicated in figure 21, the TOPMS flight-test crew consisted of a Pilot Flying who controlled the airplane from the left seat of the TSRV regular flight deck, a TOPMS Pilot who monitored the TOPMS displays in the research flight deck and communicated with the Pilot Flying by the intercom, and a Safety Pilot who occupied the right seat in the TSRV regular flight deck and participated minimally in the

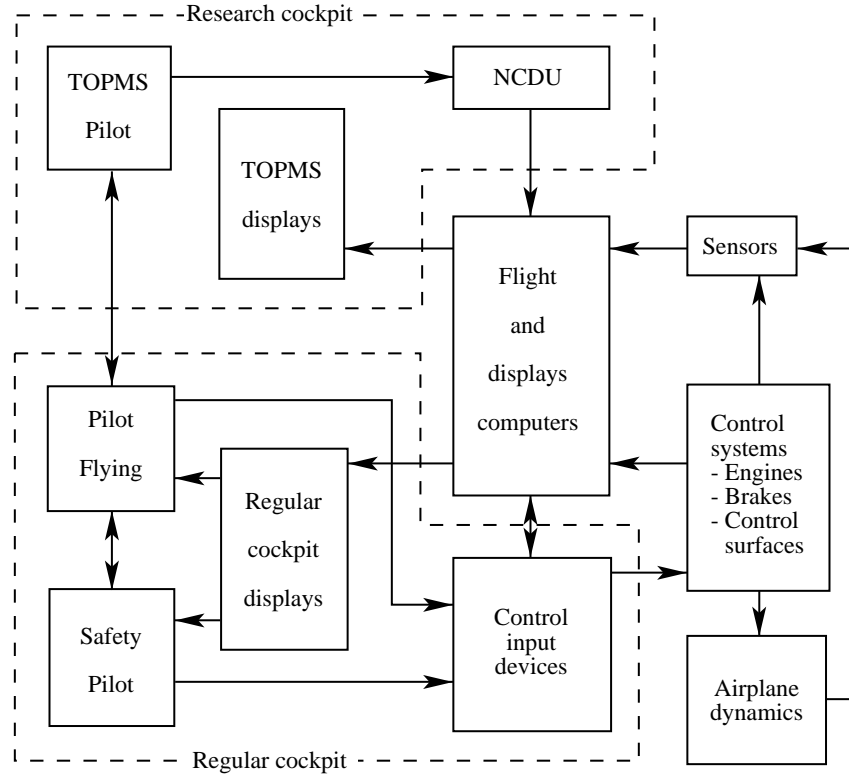


Figure 21. Functional block diagram of test system.

test program. (During a checkout flight, a 4-in monitor was temporarily mounted in the center console of the TSRV regular flight deck for the Safety Pilot to observe; however, it was too small to be useful and was removed before the actual test flights began.)

### Acceleration Measurements

Three airplane along-track acceleration signals were available of which one was selected for input to the algorithm during the test and two reference accelerations were generated by the algorithm. During pretakeoff, a nominal acceleration curve for  $\mu_r = 0.015$  (fig. 6) was generated for initial predictions of where particular performance events would occur based on existing and/or expected conditions. Then, during the takeoff roll, a reference acceleration curve was generated to reflect input deviations such as higher or lower than nominal throttle setting, wind, and  $\mu_r$  updates.

During the six days of testing, measured along-track acceleration signals were obtained from the airplane inertial measuring unit (IMU), which was available during the first three test days; an air data and inertial reference system (ADIRS), which replaced the IMU for part of the fourth test day; and the airplane body-mounted  $x$ -axis accelerometer,

which was available for all test days but was used as a TOPMS input only during the last 2.5 test days. Pitch compensation was appropriately added to each of the measured along-track acceleration signals to account for the  $1^\circ$  inclination of the TSRV body  $x$ -axis to the runway surface and to accommodate the takeoff rotation.

After a few runs on the fourth test day (table IV), the ADIRS along-track acceleration signal was discarded in favor of the body-mounted  $x$ -axis acceleration signal. As is discussed later in “Results,” the along-track acceleration signal from the TSRV ADIRS unit was found to be atypical of the high-quality, filtered acceleration signals available on modern airplanes.

Before the actual test runs, the TSRV was taxied at moderate speed down a runway at the Wallops Flight Facility while the Safety Pilot called off 1000-ft-to-go markers as the airplane physically passed them; the TOPMS Pilot, having no outside view, made similar calls when he observed the nose of the TOPMS airplane symbol pass corresponding 1000-ft tick marks along the edge of the runway graphic. The correlation was good; consequently, the test series proceeded as planned. A second opportunity for this type of calibration check occurred at the

Patrick Air Force Base on the third test day. Those results were similarly good.

### Test Runs

Eighty-five test runs (55 takeoff and 30 abort situations) were made with the TSRV. The test conditions and runs are summarized in table IV.

In addition to the test situations listed in table IV, incorrect and inconsistent data were intentionally entered for the pretakeoff calculations to demonstrate that the algorithm was configured to detect unscheduled flap settings, out-of-range or inconsistent inputted data, and runway lengths that were less than the minimum required for the takeoff. Erroneous data were purposely entered at the beginning of each test day; the resulting TOPMS displays (figs. 9 and 10) were observed several times by the TOPMS Pilot.

Because of tire and brake wear and the potential dangers associated with high-speed aborts, the flight test situations were designed so that most of them were terminated as takeoffs. For example, after an abort SAF (STOP sign) appeared for several seconds during deficient acceleration runs created by full deployment of spoilers during the takeoff roll, the Test Director declared an end to the run; the Pilot Flying lowered the spoilers and completed a preplanned takeoff. In situations which simulated engine failures, the STOP sign appeared and was observed briefly by the TOPMS Pilot who then instructed the Pilot Flying to complete another preplanned takeoff. As a consequence of such test procedures, the symbology for takeoff-roll and abort situations was sufficiently exercised and observed by the TOPMS Pilot. All TOPMS displays were recorded on videotape, but very few complete sets of numerical test data were obtained.

### Data Analysis and Results

The primary results from the TOPMS flight tests were observations of the display responses to various operational and environmental conditions. The displays were monitored in real time by all three authors and by the TOPMS Pilot who provided the evaluation comments that follow.

#### Comments by TOPMS Project Pilot

In the opinion of the TOPMS Pilot who had served as the TOPMS Project Pilot since the beginning of the simulation evaluation studies (refs. 9, 10, and 12), a highly successful transfer of TOPMS

technology was made from the TSRV B-737 simulator to the TSRV airplane. The pilot further indicated that the displays observed in this study performed like those evaluated in the simulation studies. Other comments and observations are paraphrased as follows:

The TOPMS on-line pretakeoff calculations that yielded the values of velocities  $V_1$ ,  $V_R$ , and  $V_2$  and scheduled EPR were done quickly and precisely. They yielded the same values as those that the Pilot Flying obtained from the TSRV flight manual for each of the various conditions. In addition, the algorithm appeared to correctly position the performance triangle on the runway graphic at the location where  $V_1$  and  $V_R$  would be reached.

During normal takeoffs, setting the throttles according to the scheduled EPR bars produced the proper accelerations needed for the analog airplane graphic to reach the shaded performance triangle at its pretakeoff-predicted location (i.e., the two triangles remained superimposed). This performance inspired confidence in the ability of the algorithm to provide good position information in off-nominal situations.

Deviations from nominal values of weight, thrust, and drag yielded the expected responses in the performance of the TOPMS analog display elements (viz., the airplane symbol, CAS line, shaded triangle, EPR bars, and continually updated stop points). In most situations, response changes could be attributed to improper throttle setting or to some other cause.

The SAF's report the algorithm overall analysis of the situation. Hopefully, the pilots would make the same GO/NO-GO decision without the aid of the SAF, although in some situations the decision might not be made as quickly. If the decision were NO-GO, the earlier in the takeoff roll that it is made, the easier and safer the abort will be.

In a sense, the SAF's act as a prompter to alert the TOPMS Pilot to quickly scan the distributed information for substantiation of the GO or NO-GO advisory before announcing a recommendation to the Pilot Flying. In turn, the Pilot Flying should be able to make an earlier and more confident decision.

Whereas the issue of providing pilots with SAF's and associated activation logic may

be somewhat controversial, the TOPMS algorithm has demonstrated flexibility in regard to if, when, and how such advisories are presented. Some or all of the SAF's can be omitted without significantly or adversely affecting the more fundamental distributed information (e.g., information on the acceleration performance trend provided by the triangles).

The amber SAF should be removed from consideration; it appears on the screen at a critical time when new advice is inappropriate.

During abort situations, transition from the takeoff display to the abort display with throttle retardation was very quick, smooth, and comprehensible. No visual continuity was lost and no mental reorientation was required.

The correlation was good between the football symbol (instantaneously predicted stop point) and perceived deceleration during both maximum- and partial-braking maneuvers.

The displays for all runs were recorded on videotape for later viewing and correlation with the recorded numerical data and oral comments.

### Acceleration Comparisons

In addition to the pilot conversations and comments, several performance variables were recorded for use in real-time and postflight analyses. These analyses involved acceleration time-history comparisons and continual determination of the airplane position on the runway based on several measurement and computational techniques.

Figure 22 shows an example of the along-track acceleration measured by the ADIRS sensor unit. Also shown is the reference acceleration that was computed by the algorithm for a normal takeoff roll under the same conditions. The ADIRS-measured acceleration signal was oscillatory within a moderately large envelope. (Subsequently it was judged to be a poor representation of the actual airplane acceleration.) This oscillation which caused some unexpected SAF display problems is illustrated in figures 22–24. The algorithm one-time adjustment of the magnitude of the reference acceleration to that of the measured acceleration came at a time (approximately 19 sec into the takeoff roll) when the ADIRS curve was in one of its valleys; consequently, the algorithm demanded a large step change in the reference acceleration curve to match that of the ADIRS-measured acceleration. Figure 23 shows an enlargement of the figure 22 curves in the adjustment region. After the

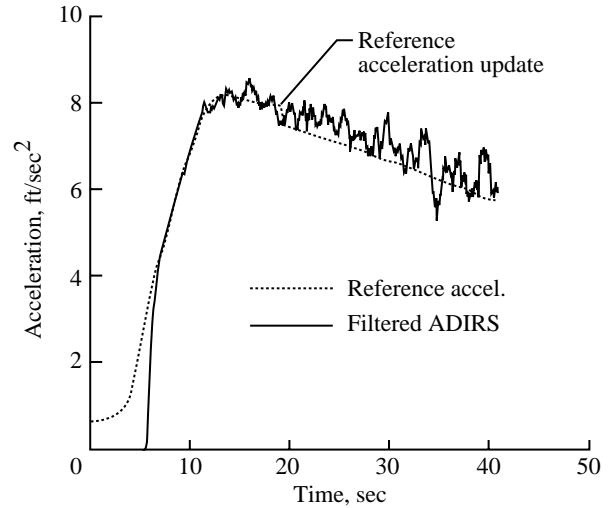


Figure 22. Comparison of TOPMS reference and ADIRS along-track-acceleration signals during normal takeoff roll.

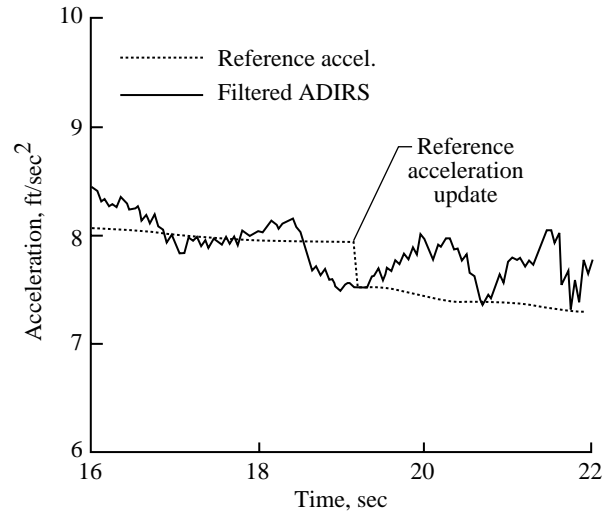


Figure 23. Enlargement of figure 22 reference acceleration adjustment.

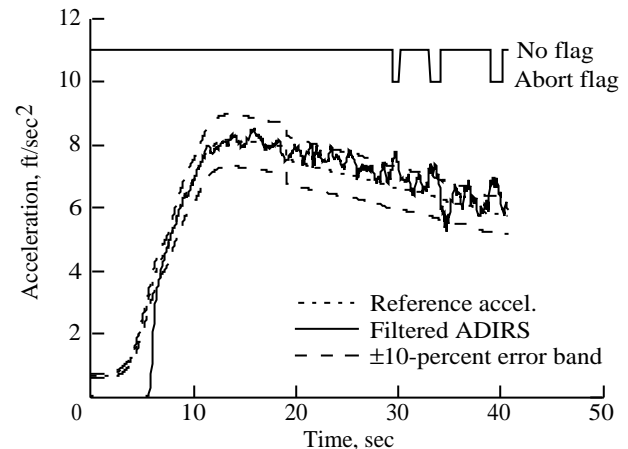


Figure 24. Abort flag occurrences due to ADIRS along-track-acceleration signal excursions outside  $\pm 10$ -percent error band ( $n = 5$ ).

step change, the reference acceleration curve continues along a path parallel to its original path (unless the throttles are again moved or an engine fails). Notice that the corrected reference curve skirts along the bottom boundary rather than through the middle of the ADIRS acceleration envelope. (See earlier discussion in “Algorithm.”)

To determine the acceptability of a particular takeoff-roll performance, a selected acceleration-error band that extends 10 percent above and below the reference acceleration curve was programmed for the flight tests. This band is shown in figure 24 for the ADIRS reference curve shown in figure 22. Observe that the measured along-track acceleration exceeded the  $\pm 10$ -percent error band of the reference acceleration several times during the course of the run. To illustrate the problem, a segment of the discrete logic signal that controlled the SAF's during the flight test in figure 22 has been merged in time across the top of figure 24. As shown, three abort SAF's flashed on for approximately 1 sec, which resulted in distraction and concern even though no actual acceleration problem existed. The videotape recorded during this run verified that three abort SAF's had appeared briefly on the display.

In figures 22 and 23, observe that had the acceleration adjustment for matchup occurred about 1 sec later, a small upward movement in the reference signal would have occurred and most likely would have shifted the upper error band high enough to preclude the three on-off abort SAF flashes. However, a large downward excursion of the ADIRS signal at approximately 34 sec (fig. 24) would probably have caused a single flash of the abort SAF.

Figure 25 shows the concurrently measured (but unused) acceleration signal from the TSRV body-mounted  $x$ -axis accelerometer during the same run. (See figs. 22–24.) Note that this signal did not have large oscillations; if it had been used as the input to the TOPMS algorithm for this run, the effect of the wind and  $\mu_r$  adjustments at 19 sec would have been hardly noticeable. Further note that if a  $\pm 10$ -percent error band had been drawn for this reference curve, the acceleration measured by the body-mounted accelerometer would have been easily contained within it.

The following two software patches, which were coded and approved by safety personnel before the flight, were temporarily installed in the TOPMS software to alleviate the nuisance SAF problem that occurred when the ADIRS acceleration measurement was used to drive the TOPMS displays:

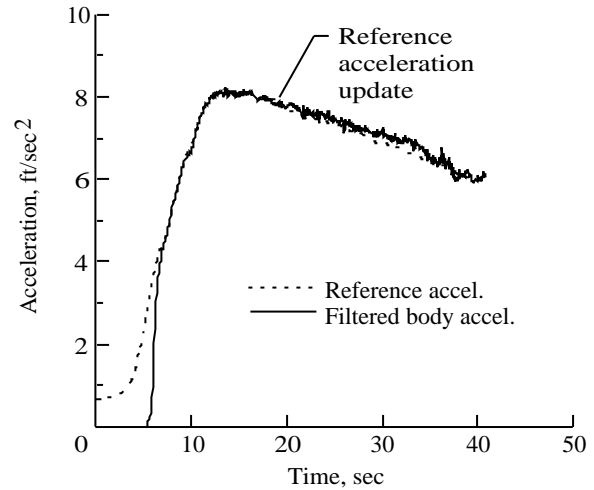


Figure 25. Comparison of TOPMS reference and TSRV body-mounted  $x$ -axis accelerations during a normal takeoff roll.

1. A digital counter prevented the appearance of an abort SAF due to out-of-range, along-track acceleration unless the signal remained out of range during several consecutive (or nearly consecutive) data samples (sample rate of 20 per sec).
2. The acceleration-error tolerance band was increased from  $\pm 10$  to  $\pm 15$  percent.

The out-of-range digital counter functioned as follows. A positive integer  $n$  was initially set to zero. When the sampled acceleration-error value exceeded the  $\pm 10$ -percent error band in a computation cycle,  $n$  advanced one count. If the acceleration signal was still out of bounds on the next computation cycle,  $n$  advanced another count; however, if the acceleration signal was back inside the error band,  $n$  was reduced one count. Experimental limits were imposed on  $n$ ; for example, if  $n = 5$  were this limit (corresponding to the acceleration signal being out of bounds for 0.25 sec), the TOPMS logic would activate an abort SAF only when  $n = 5$ . It would remain at  $n = 5$  until the acceleration signal was again within bounds, whereupon  $n$  would drop back one count toward zero. When  $n = 0$ , it remained there unless another excursion occurred. The  $n$  values investigated were 5, 8, and 10. This technique yielded improved results but did not eliminate all the SAF nuisance flashing, even when  $n$  was set at 10.

The second software patch expanded the acceleration-error band from  $\pm 10$  to  $\pm 15$  percent, which would easily have contained the ADIRS acceleration signal shown in figures 22–24. Together the two fixes eliminated the nuisance SAF's triggered by the ADIRS signal; the second fix alone probably would have been sufficient and was certainly

the most straightforward. In retrospect, the revised  $\pm 15$ -percent limit may be just as appropriate as the arbitrarily selected  $\pm 10$ -percent limit. However, if an airplane is equipped with a sensor package that delivers a reasonably well-filtered along-track acceleration signal, the smaller band should be sufficient. Defining an optimal acceleration-error band was beyond the scope of this investigation.

Figure 26 shows measured and reference acceleration for a situation in which the spoilers were intentionally deployed from the beginning of the takeoff roll. Note that as speed increased, the measured acceleration fell below the reference curve (dashed line) as expected. When the algorithm made its check of the acceleration performance just after the throttles were set for 3 sec, the measured acceleration was about  $0.5 \text{ ft/sec}^2$  below what it nominally should have been for the measured throttle setting. Accordingly, the algorithm changed  $\mu_r$  and adjusted the reference acceleration to the measured value at this time. Subsequently, the abnormally increasing aerodynamic drag due to the deployed spoilers continued to cause the measured acceleration to decrease. At about 21 sec, the algorithm determined that the measured acceleration error had exceeded the  $\pm 10$ -percent limit and it switched on the abort SAF. After the TOPMS Pilot briefly observed the SAF, the run was declared complete and the Pilot Flying lowered the spoilers and made a preplanned takeoff.

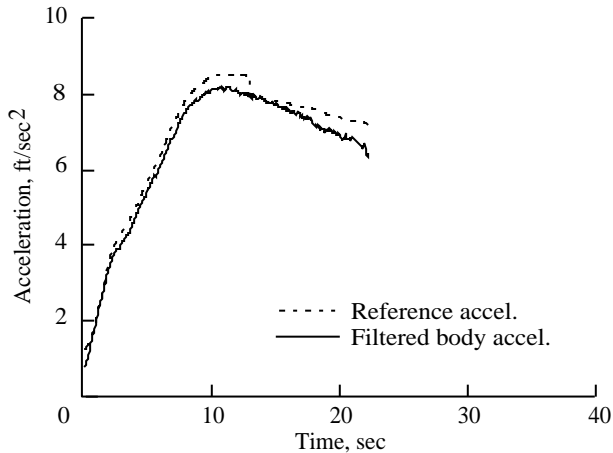


Figure 26. Comparison of reference and body-mounted  $x$ -axis acceleration signals during takeoff with excess drag (deployed spoilers).

### Distance Determination Using Alternative Methods

The TOPMS algorithm computed the TSRV runway positions throughout the flight-test series by

double integration of the pretakeoff-predicted (nominal) and the real-time-measured (and filtered) accelerations. (See fig. 7.) The TSRV positions were referenced to a specified start point whose coordinates were preestablished by land survey. During postflight analysis, filtration and single integration of the independently measured ground speed (method 2 in fig. 7) appeared to provide more accurate runway positioning. This was determined by comparing distances-traveled data obtained by single integration of ground speed, by double integration of acceleration, and by real-time range measurements made with the Wallops Flight Facility ground-based laser tracker. This tracker has a dynamic range accuracy of  $\pm 1.65 \text{ ft}$  (standard deviation) and a pointing accuracy of  $0.3 \text{ mrad}$  in azimuth. (See ref. 14.) Unfortunately, the laser tracker was available for only part of one test day.

Because of the variability of flight-test conditions and procedures (including early termination of some runs and/or early cutoffs of data recorders), only six normal takeoff runs had sufficiently complete data sets for strict comparisons of the TSRV positions at  $V_R$ ; the TSRV was tracked by laser radar in only two of these runs, which further restricted comparative data. These data are shown in table V.

Table V. Measured and/or Computed Positions of TSRV at  $V_R$

Run	Distance, ft			
	$^*d_p$	$^\dagger d_a$	$^\ddagger d_{gs}$	$^l d_{lt}$
1	3307	$\parallel 3033$	3068	
2	3441	$\parallel 3467$	3740	
3	3244	$\parallel 3067$	3248	
4	3133	$\# 2909$	3140	
5	2637	$\# 2452$	2631	2690
6	2645	$\# 2427$	2634	2696

$^*d_p$ , algorithm-predicted distance from nominal acceleration.

$^\dagger d_a$ , algorithm-computed distance from measured acceleration.

$^\ddagger d_{gs}$ , algorithm-computed distance from measured ground speed.

$^l d_{lt}$ , measured distance from radar laser tracker.

$\parallel$  Acceleration signal from IMU.

$\#$  Acceleration signal from body-mounted accelerometer.

Runs 1–3 show results when the along-track acceleration input to the TOPMS algorithm came from the TSRV IMU. Runs 4–6 show similar data when the input was obtained using the body-mounted,  $x$ -axis accelerometer. No suitable along-track acceleration input signals were obtained from the ADIRS unit.



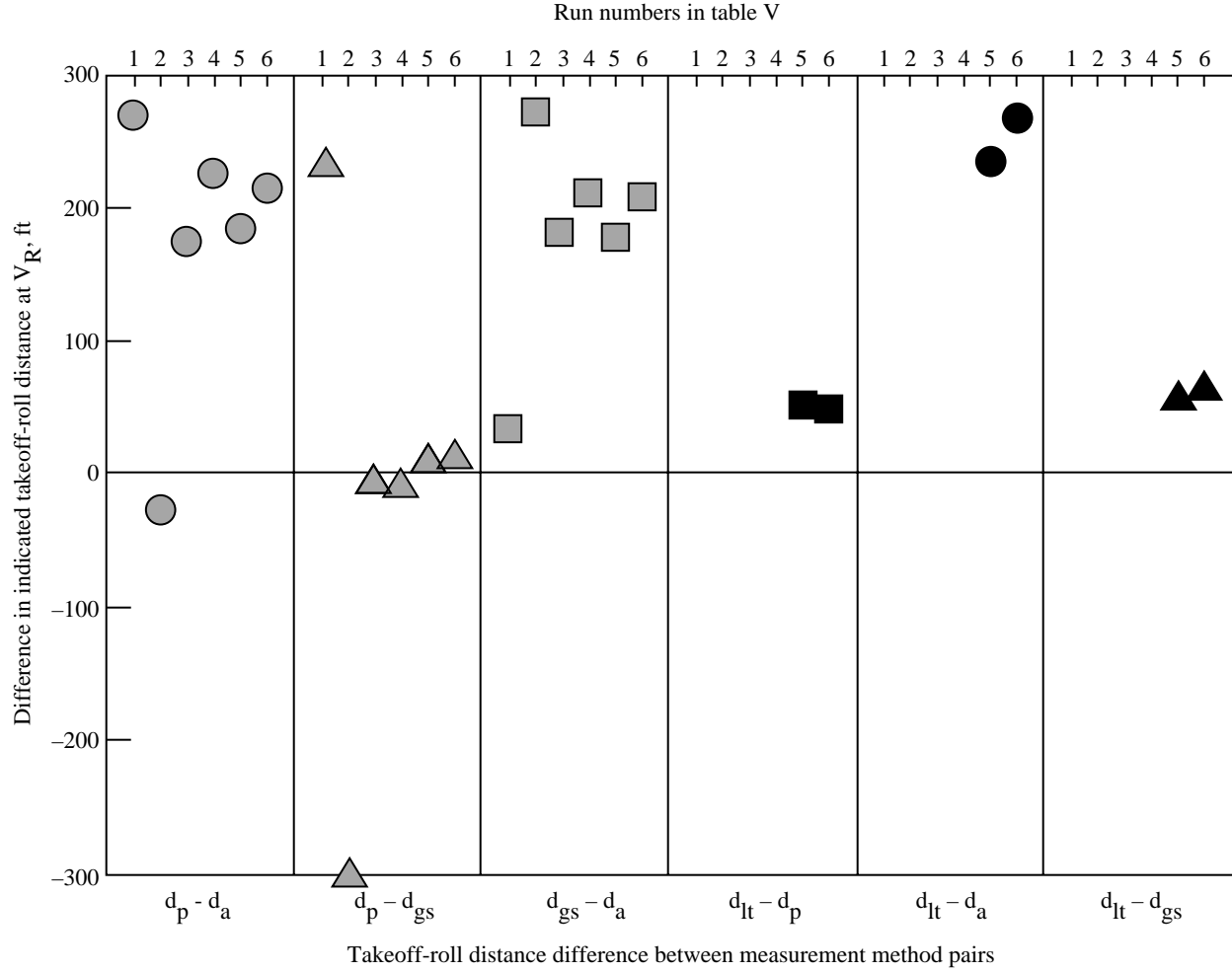


Figure 27. Comparison of laser-tracker-measured and TOPMS-computed positions of TSRV at  $V_R$ .

A comparison of the computed and measured position data is shown in figures 27–29). In figure 27, six groups of incremental differences in takeoff-roll distances are shown across the bottom and the run numbers common to each group are indicated along the top. With the exception of run 2, the algorithm method 1 computed values of takeoff-roll distances  $d_a$  from the TSRV start points to the locations where its airspeed reached  $V_R$  were approximately 200 ft less than pretakeoff-roll-predicted distances  $d_p$  for nominal conditions. The magnitude of the differences corresponds roughly to two lengths of the TSRV or less than the distance it travels during the last second before reaching  $V_R$ . Part of the difference can be attributed to  $\mu_r$  being updated from the 0.015 assumed nominal value to values ranging from 0.020 to 0.030. Also, the wind inputs were adjusted 2–3 knots upward in all but run 2, where no change occurred. In runs 3–6, the method 2 computations of distance traveled for the TSRV to reach  $V_R$  ( $d_{gs}$ ) closely agreed with pretakeoff predictions of  $V_R$  positions; method 1 computations showed only fair agreement.

Runs 1 and 2 provided mixed support of this trend. In runs 5 and 6,  $d_p$  and  $d_{gs}$  compared well with the respective laser-tracker measurements ( $d_{lt}$ ).

To provide additional insight, figures 28 and 29 present curve data of the TSRV runway positions during runs 5 and 6, respectively, by using the computational methods 1 and 2. In figure 28, the run 5 pretakeoff prediction (2637 ft) of where the TSRV should reach a speed of  $V_R$  under nominal conditions is indicated by the dark circle. The laser-tracker-measured distance at  $V_R$  (2690 ft) is indicated by the triangle. The solid and dashed lines show corresponding positions using integration methods 1 and 2, respectively. Both curves end at the location where CAS reaches  $V_R$ . Similar data for run 6 are shown in figure 29. Both sets of curves appear to increase smoothly with airspeed, indicating that the distance differences might be attributable to the integration methods rather than any parameter-correction anomalies. However, not enough data are available to confirm the trend.

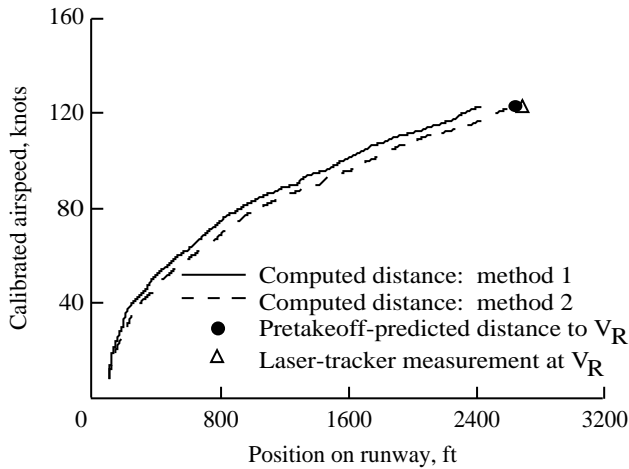


Figure 28. Comparison of laser-tracker-measured and three computed positions of TSRV during run 5 takeoff roll.

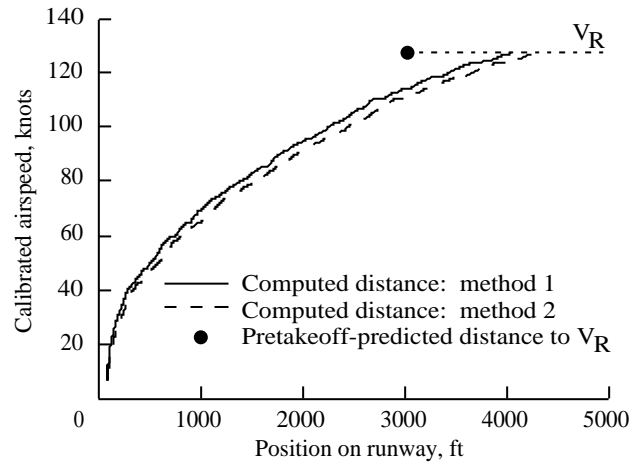


Figure 30. Comparison of runway position computation methods 1 and 2 during reduced-thrust takeoff run.

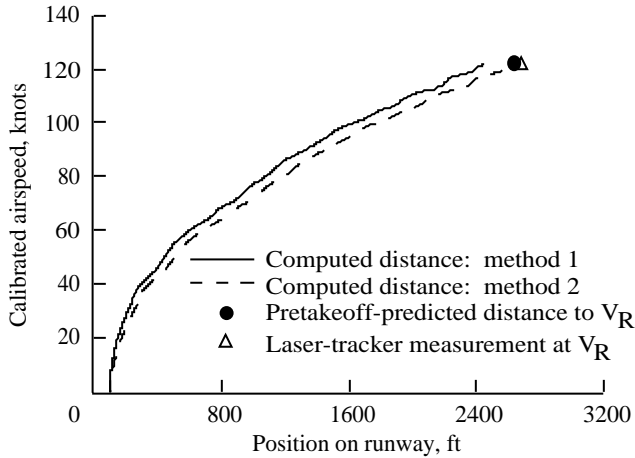


Figure 29. Comparison of laser-tracker-measured and three computed positions of TSRV during run 6 takeoff roll.

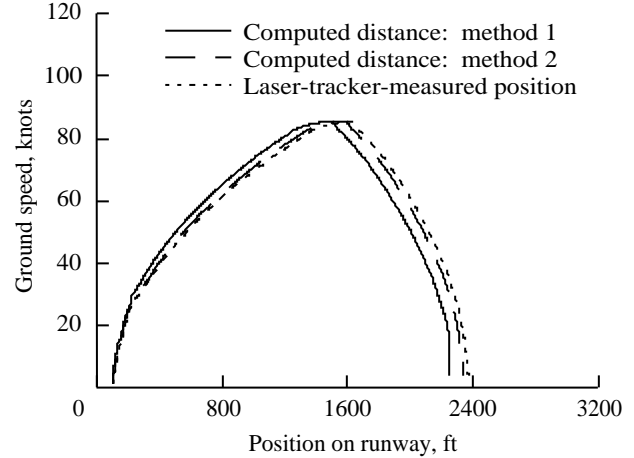


Figure 31. Roll distances before and braking distances after abort at 80 knots.

The method 1 versus method 2 pattern was also apparent during a reduced-thrust takeoff from the 2000-ft-altitude commercial runway at Asheville, North Carolina, where no laser tracker was available. (See fig. 30.) The circle at approximately 3000 ft down the runway shows the pretakeoff prediction based on the throttle setting that would produce a scheduled EPR of 1.95. However, during this run, the pilot purposely used a throttle setting that produced an EPR of 1.7. The resulting lower acceleration level caused the CAS to increase at a slower pace and, according to method 1, the TSRV reached  $V_R$  about 1000 ft farther down the runway than predicted at pretakeoff; when using method 2, the TSRV position was about 1200 ft farther down the runway. (Both curves terminate where CAS reaches  $V_R$ .)

### Aborted Takeoffs

Two maximum-braking aborts were made during tests at the Wallops Flight Facility. The primary purpose was to compare the laser-tracker-measured stopping distances versus the stopping distances computed by the TOPMS algorithm using methods 1 and 2. Figures 31 and 32 show this comparison for maximum-braking stops from approximately 80 knots and 100 knots, respectively. The winds were light for both runs so the CAS and ground-speed values were approximately equal.

At the beginning of the 80-knot situation (fig. 31),  $\mu_r = 0.04$  was entered as an intentional error, which the algorithm corrected to  $\mu_r = 0.016$  at approximately 30 knots. At 80 knots, it took about 3 sec

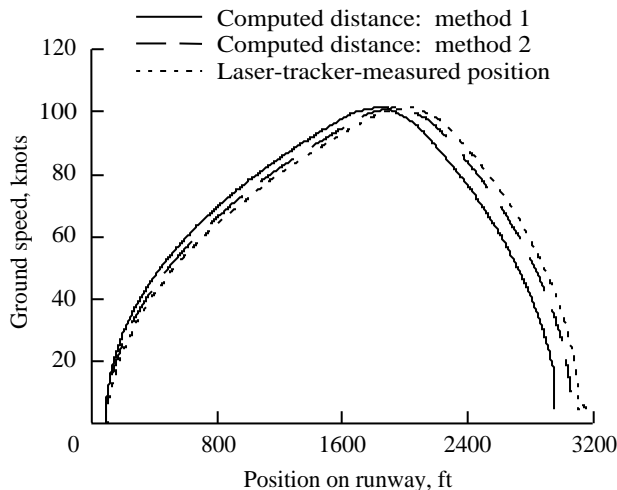


Figure 32. Roll distances before and braking distances after abort at 100 knots.

for the TOPMS Pilot to call for the abort and for the Pilot Flying to respond (i.e., hear the call, reduce the throttles, pull the speed-brake lever, and apply the foot brakes); consequently, ground speed reached approximately 86 or 87 knots before braking became the dominant longitudinal force. A comparison of airplane position during the takeoff roll showed the same trend as seen during previous takeoffs (figs. 28 and 29); that is, the laser tracker determined that the position of the airplane was ahead of the TOPMS-computed position. Note that the TOPMS computations and the laser measurements of the braking distance correlated closely; the distance differential at the end of the run was about the same as it had been at abort initiation. (The runs were declared complete when speed was reduced to about 15 knots because the TSRV antiskid brake system ceased operation below this level.)

In the 100-knot situation, the Pilot Flying reacted more quickly (in slightly less than 2 sec) and ground speed reached only about 103 knots when full braking was applied. Laser tracker measurements and method 2 computations of braking distance agreed closely; again, the laser tracker indicated that the TSRV was slightly farther down the runway.

To add interest during another braking run at the Wallops Flight Facility, the TOPMS Pilot covertly selected the 2000-ft-to-go mark on his runway graphic as a target stop point. Then without informing the Pilot Flying of the purpose, the TOPMS Pilot verbally instructed the Pilot Flying when to apply more or less braking. The Pilot Flying obliged and the TSRV was brought to a stop as the nose of the graphic airplane reached the target mark. The TOPMS Pilot then asked the Safety Pilot to look out

the side window and report where the airplane had stopped. The TSRV had indeed come to a stop approximately opposite the 2000-ft-to-go marker sign alongside the runway. Although this was not a planned or rigorous test, it further demonstrated that the TOPMS algorithm was providing reasonably accurate distance information on dry runway surfaces.

## Additional Discussion of TOPMS Displays

The SAF's and predicted stop point  $\times$  augment the elemental, distributed TOPMS display with important information concerning both system and acceleration performance. For example, after an engine failure, the pilot must quickly assess the seriousness of the situation and decide whether the airplane can be stopped in the remaining runway distance. A red SAF would instantly advise the pilot that the airplane could probably be stopped; a green SAF would indicate that it most likely could not. The predicted stop-point symbol  $\times$  would support the SAF in both cases.

An EPR bar that rises to its target (scheduled) mark, turns red, and does not diminish in length indicates a serious mismatch between the measured EPR and the EPR value associated with the measured throttle position. A situation in which both engines are operating with a serious EPR mismatch is illustrated in figure 19. In this figure, the shaded triangle has advanced so far downfield that it has crossed the GRLL. Two violations of TOPMS criteria that have occurred (table IV) for continued takeoff are a large EPR versus throttle-position EPR disagreement and insufficient runway distance remaining for a sanctioned takeoff. Either of these violations would trigger an abort SAF. The following real-world case (ref. 15) illustrates this situation.

In January 1982, a heavily loaded Boeing 737-222 transport attempted to depart from the Washington National Airport in a heavy snowstorm. For several contributing reasons, the flight ended in a fatal crash soon after liftoff. The runway length was near minimum for the airplane under the existing weather and loading conditions.

If a TOPMS like the one described in this report had been operating aboard that aircraft, it would have provided the pilots with the following information:

1. Before beginning the takeoff roll, the pilot would have set the throttles on zero deflection angle for idle thrust, but the EPR bars on the display would have extended noticeably above their usual zero length, which indicates that greater

than idle thrust was being sensed. Engine sound and other cockpit information, however, would not have supported an above-idle-thrust situation and would have alerted the crew of a potentially serious problem.

2. If this visual cue were ignored and the takeoff roll begun, both EPR bars would have risen to their respective target marks in response to the throttle advances, which would have been lower than normal. About 3 sec after the throttles were set to match the target EPR marks on the display, both EPR bars would have turned red but retained their target length. Additionally, the algorithm would have reacted to the large mismatch between the target EPR and the EPR value associated with the sensed throttle position by immediately causing an abort SAF and a predicted stop-point  $\times$  to appear on the runway graphic. The shaded triangle would also have jumped far down the runway indicating that measured acceleration was significantly lower than the nominal expected for the ongoing maneuver.
3. If the takeoff roll continued, the shaded triangle would have soon crossed the GRLL (shown in fig. 19), violating yet another abort criterion. (See condition 7 in table III.)

A TOPMS display with lesser features (e.g., no SAF or  $\times$ ) would also have provided valuable information in the case described above but would not have been as dramatic. The nominal-length red EPR bars would have brought attention to the display; the greatly separated triangles would have graphically pointed out the magnitude of the low-acceleration condition and the fact that the airplane might not attain  $V_R$  before it reached the GRLL.

Inclusion of the SAF's in the TOPMS package is not intended to reduce pilot responsibility in deciding on a course of action (i.e., GO or NO-GO). The SAF's provide an instant second opinion that a problem that requires action may exist based on the algorithm's logical analysis of existing parametric values and other data related to programmed criteria. Whereas the SAF's may not be perceived as top-priority (or necessary) information by highly experienced pilots (such as the TOPMS Pilot in this study), the SAF's would provide valuable and timely cues for less experienced pilots; the SAF's would prompt them to immediately scan the supporting information to ascertain or verify a real or potential problem and quickly decide on the appropriate control response (i.e., make the GO/NO-GO decision as early as possible).

An alternative to the abort SAF in this situation could be an acceleration-error indicator (e.g., the one used in the TOPMS head-up display in the ref. 16 simulation study). Inclusion of either the abort SAF or an acceleration-error indicator should facilitate early investigation of the cause of the shaded triangle displacement away from the predicted  $V_R$  point (i.e., lower than nominal throttle setting, EPR-bias errors, or excessive drag). The presence of either symbol (or both) also relieves the pilot from having to closely or continuously watch the shaded triangle.

For completeness, the amber SAF (table III and fig. 16) was flight tested; however, it is being deleted from the TOPMS for lack of sufficient pilot support in this and in previous studies. (See ref. 11.)

## Concluding Remarks

The Langley Takeoff Performance Monitoring System (TOPMS) is a computer software and hardware graphics system that visually displays current runway position, acceleration performance, engine status, and other situation advisory information to aid pilots in their decision to continue or to abort a takeoff. The TOPMS was successfully installed and tested on the Transport System Research Vehicle (TSRV), a highly modified Boeing 737-100 research airplane. The navigation screen in the TSRV research flight deck displayed TOPMS information while the TSRV was on the runway; at liftoff, the TOPMS display disappeared and normal navigation information automatically returned to this screen. Six days of runway testing consisting of 85 takeoff or abort situations were conducted at five airfields between March 1987 and November 1989.

The TOPMS runway tests indicated to the test team that the simulator-developed TOPMS technology had been successfully transferred to the TSRV. The algorithm was easily installed on the TSRV regular graphics computer. It reliably calculated the TSRV performance and accurately provided a graphical display of the runway situation expected under a variety of nominal and error conditions (i.e., induced acceleration deficiencies; simulated engine failures; and several runway, gross-weight, temperature, wind, pressure, altitude conditions). The TOPMS also interfaced well with other onboard equipment through the airplane all-purpose, high-speed data bus.

Although quantitative data gathering was not a primary test objective, some preliminary distance comparisons were extracted from recorded flight data. In particular, the following trends were observed:

1. When roll distances required to reach takeoff speed  $V_R$  were computed from accelerometer measurements, they were typically two airplane lengths less than (a) pretakeoff-predicted distances computed from nominal acceleration, (b) distances measured by a ground-based laser radar tracker, and (c) distances computed from independently measured ground speed.
2. The computed and measured braking distances appeared to be in better agreement than the takeoff-roll distances; however, additional data are needed to confirm this.

Based on the results of these runway tests, the following recommendations concerning the TOPMS algorithm and displays are listed:

1. A study should be made to determine the optimal magnitude of the error band about the reference acceleration to prevent unwarranted or nuisance abort advisories. This study illustrated that a  $\pm 10$ -percent error band should be sufficient when well-filtered, along-track accelerometer signals are available; however, this error band may not adequately encompass all of the possible nuisance anomalies.
2. The  $\mu_r$ -update feature could be removed because it appears to provide very little practical

benefit; in fact, in some instances, it may be counterproductive.

3. The GO and NO-GO SAF's should be retained as active elements of the TOPMS displays. The TOPMS displays provide desirable basic performance information without them, but they appear to be a positive enhancement.
4. A good-quality measured ground-speed signal when available on a particular airplane, should be considered as the TOPMS input for the real-time distance computation of the airplane position. This computational technique, however, also needs more extensive study.

The TOPMS is operational and has been retained on the TSRV for general use and demonstration. It would, however, be desirable to demonstrate and evaluate the TOPMS on another airplane with different characteristics, sensors, and support equipment (e.g., a head-up display). The TOPMS software could be adapted and used to advantage on any modern airplane equipped with digital flight-control computers.

NASA Langley Research Center  
Hampton, VA 23681-0001  
February 16, 1994

## References

1. Bacqué, Peter: NASA Offers Airline Pilots Aid. *Richmond Times-Dispatch*, Sunday, Nov. 12, 1989, p. C-8.
2. Minutes of Meeting #1 of the Take-Off Performance Monitoring Ad Hoc Committee. Aircraft Div., Aerospace Council, Soc. of Automotive Engineers, Inc. (Washington, D.C.), May 15-16, 1984.
3. Fusca, James A.: Takeoff Monitor Computes Runway Roll. *Aviat. Week & Space Technol.*, vol. 69, no. 15, Oct. 13, 1958, pp. 99-100 and 103-105.
4. Compania de Transport Aerian Tarom (Ioan Aron and Ion Tomescu): Take-Off Director System. U.S. Patent No. 4,251,868, Feb. 17, 1981.
5. Small, John T., Jr.: Feasibility of Using Longitudinal Acceleration ( $N_x$ ) for Monitoring Takeoff and Stopping Performance From the Cockpit. *The 1983 Report to the Aerospace Profession—27th Symposium Proceedings*, vol. 18, no. 4, Soc. of Experimental Test Pilots, 1983, pp. 143-154.
6. Boeing Co. (Patrick J. Cleary, Lloyd S. Kelman, and Richard L. Horn): Aircraft Performance Margin Indicator. European Patent Appl. No. 85200977.8, Publ. No. 0 166 487 A2, June 19, 1985.
7. Srivatsan, R.: Design of a Takeoff Performance Monitoring System. Ph.D. Thesis, Univ. of Kansas, 1985.
8. Srivatsan, R.; Downing, D. R.; and Bryant, W. H.: *Development of a Takeoff Performance Monitoring System*. NASA TM-89001, 1986.
9. Middleton, David B.; Srivatsan, Raghavachari; and Person, Lee H., Jr.: *Simulator Evaluation of a Display for a Takeoff Performance Monitoring System*. NASA TP-2908, 1989.
10. Middleton, David B.; Srivatsan, Raghavachari; and Person, Lee H., Jr.: Simulator Evaluation of Takeoff Performance Monitoring System Displays. *A Collection of Technical Papers—AIAA Flight Simulation Technologies Conference*, Sept. 1988, pp. 206-214. (Available as AIAA-88-4611-CP.)
11. *Airworthiness Standards: Transport Category Airplanes*. FAR Pt. 25, Federal Aviation Adm., June 1974.
12. Middleton, David B.; Srivatsan, Raghavachari; and Person, Lee H., Jr.: *Simulator Evaluation of Displays for a Revised Takeoff Performance Monitoring System*. NASA TP-3270, 1992.
13. Bruce, Kevin R.: *NASA B737 Flight Test Results of the Total Energy Control System*. NASA CR-178285, 1987.
14. Staff of NASA Langley Research Center and Boeing Commercial Airplane Co.: *Terminal Configured Vehicle Program—Test Facilities Guide*. NASA SP-435, 1980.
15. *Aircraft Accident Report—Air Florida, Inc., Boeing 737-222, N62AF Collision With 14th Street Bridge, Near Washington National Airport, Washington, D.C.*, January 13, 1982. NTSB-AAR-82-8, Aug. 10, 1982. (Available from NTIS as PB 82 910 408.)
16. Middleton, David B.; Srivatsan, Raghavachari; and Person, Lee H., Jr.: Takeoff Performance Monitoring System Display Options. *A Collection of Technical Papers—AIAA/AHS Flight Simulation Technologies Conference*, Aug. 1992, pp. 57-67. (Available as AIAA-92-4138.)

<b>REPORT DOCUMENTATION PAGE</b>			Form Approved OMB No. 0704-0188	
Public reporting burden for this collection of information is estimated to average 1 hour per response, including the time for reviewing instructions, searching existing data sources, gathering and maintaining the data needed, and completing and reviewing the collection of information. Send comments regarding this burden estimate or any other aspect of this collection of information, including suggestions for reducing this burden, to Washington Headquarters Services, Directorate for Information Operations and Reports, 1215 Jefferson Davis Highway, Suite 1204, Arlington, VA 22202-4302, and to the Office of Management and Budget, Paperwork Reduction Project (0704-0188), Washington, DC 20503.				
<b>1. AGENCY USE ONLY (Leave blank)</b>		<b>2. REPORT DATE</b> May 1994	<b>3. REPORT TYPE AND DATES COVERED</b> Technical Paper	
<b>4. TITLE AND SUBTITLE</b> Flight Test of Takeoff Performance Monitoring System			<b>5. FUNDING NUMBERS</b>  WU 505-64-13-04	
<b>6. AUTHOR(S)</b> David B. Middleton, Raghavachari Srivatsan, and Lee H. Person, Jr.				
<b>7. PERFORMING ORGANIZATION NAME(S) AND ADDRESS(ES)</b> NASA Langley Research Center Hampton, VA 23681-0001			<b>8. PERFORMING ORGANIZATION REPORT NUMBER</b>  L-17274	
<b>9. SPONSORING/MONITORING AGENCY NAME(S) AND ADDRESS(ES)</b> National Aeronautics and Space Administration Washington, DC 20546-0001			<b>10. SPONSORING/MONITORING AGENCY REPORT NUMBER</b> NASA TP-3403	
<b>11. SUPPLEMENTARY NOTES</b> Middleton and Person: Langley Research Center, Hampton, VA; Srivatsan: ViGYAN, Inc., Hampton, VA.				
<b>12a. DISTRIBUTION/AVAILABILITY STATEMENT</b>  Unclassified-Unlimited  Subject Category 08			<b>12b. DISTRIBUTION CODE</b>	
<b>13. ABSTRACT (Maximum 200 words)</b> The Takeoff Performance Monitoring System (TOPMS) is a computer software and hardware graphics system that visually displays current runway position, acceleration performance, engine status, and other situation advisory information to aid pilots in their decision to continue or to abort a takeoff. The system was developed at the Langley Research Center using the fixed-base Transport Systems Research Vehicle (TSRV) simulator. (The TSRV is a highly modified Boeing 737-100 research airplane.) Several versions of the TOPMS displays were evaluated on the TSRV B-737 simulator by more than 40 research, United States Air Force, airline and industry and pilots who rated the system satisfactory and recommended further development and testing. In this study, the TOPMS was flight tested on the TSRV. A total of 55 takeoff and 30 abort situations were investigated at 5 airfields. TOPMS displays were observed on the navigation display screen in the TSRV research flight deck during various nominal and off-nominal situations, including normal takeoffs; reduced-throttle takeoffs; induced-acceleration deficiencies; simulated-engine failures; and several gross-weight, runway-geometry, runway-surface, and ambient conditions. All tests were performed on dry runways. The TOPMS software executed accurately during the flight tests and the displays correctly depicted the various test conditions. Evaluation pilots found the displays easy to monitor and understand. The algorithm provides pretakeoff predictions of the nominal distances that are needed to accelerate the airplane to takeoff speed and to brake it to a stop; these predictions agreed reasonably well with corresponding values measured during several fully executed and aborted takeoffs. The TOPMS is operational and has been retained on the TSRV for general use and demonstration.				
<b>14. SUBJECT TERMS</b> Takeoff; Takeoff performance; Takeoff performance monitoring system; TOPMS; Flight tests; GO/NO-GO; Aborted takeoff; Rejected takeoff; Cockpit displays; Electronic displays; Pilot evaluation			<b>15. NUMBER OF PAGES</b> 28	
			<b>16. PRICE CODE</b> A03	
<b>17. SECURITY CLASSIFICATION OF REPORT</b> Unclassified	<b>18. SECURITY CLASSIFICATION OF THIS PAGE</b> Unclassified	<b>19. SECURITY CLASSIFICATION OF ABSTRACT</b>	<b>20. LIMITATION OF ABSTRACT</b>	